Independent Domestication of a Tailed Bacteriophage into a Killing Complex in *Pseudomonas*.

Running title: Phage-derived bacteriocins in *Pseudomonas syringae*

Kevin L. Hockett[1], Tanya Renner[2],[3], and David A. Baltrus[1]

[1]School of Plant Sciences, University of Arizona, Tucson, AZ 85721-0036, U.S.A.; [2]Department of Entomology and the Center for Insect Science, University of Arizona, Tucson, AZ 85721, U.S.A.; [3]Biology Department, San Diego State University, San Diego, CA 92182, U.S.A.

Abstract

Competition between microbes for limiting resources is widespread in nature. The strength of competition is often positively correlated with relatedness between microbes (intraspecific) as overlapping metabolism negate opportunities for niche partitioning. Bacteria have evolved numerous protein-based systems, collectively referred to as bacteriocins, that provide a fitness advantage during direct competition because they specifically kill strains or species closely related to the producer. This includes small, posttranslationally modified peptides, large, unmodified proteins, and domesticated tailed bacteriophages. In this work we sought to characterize bacteriocin genetic complements and killing spectra across the phylogenetic breadth of *Pseudomonas syringae*, an important phytopathogen. In characterizing the killing spectra for the model strain *P. syringae* B728a, we discovered its activity could not be explained by the presence of predicted bacteriocins. Using a reverse genetic approach, whereby we identified candidate bactericidal factors based on the presence of SOS-response transcriptional regulators, we found that the killing activity is derived from a prophage region. Despite this region being described nearly a decade ago, and numerous comparative genomic studies aimed at understanding evolution across this species, the ecological role of this region has remained elusive. This region does not encode an active prophage (i.e. one that will give rise to a replicative bacteriophage), but rather a bacteriophage-derived bacteriocin, termed an R-type syringacin. The R-type syringacin, is striking in its convergence with the well-studied R-type pyocin of *P. aeruginosa* in both synteny and molecular function. Multiple lines of evidence, including genomic alignment, amino acid percent sequence identity, and phylogenetic inference all support the conclusion of the R-type syringacin being derived independently of the R-type pyocin. Moreover, we demonstrate that this region is conserved, though not strictly syntenic, among several other *Pseudomonas* species, including *P. fluorescens*, *P. protegens*, *P. chlororaphis*, and *P. putida*, and thus is likely important for intermicrobial interactions throughout this important genus.

Introduction

The genus *Pseudomonas* includes organisms exhibiting diverse ecological strategies and life histories, including human and plant pathogens, plant mutualists, as well as saprotrophic plant, soil, and water inhabiting organisms (Lugtenberg & Bloemberg 2004; Sørensen & Nybroe 2004; D'Argenio 2004; Hirano & Upper 2000; Morris et al. 2008; Morris et al. 2010). Many of the environments inhabited by this genus are limited in available forms of one or several key nutrients (e.g. carbon or nitrogen), which drives intermicrobial competition (Wilson & Lindow 1994a; Demoling et al. 2007; Harrison 2007). While other habitats are relatively replete with nutrients, the distribution of microbes can be spacially limited which drives competition for colonization of particular anatomical locations (Lugtenberg & Kamilova 2009). Resource competition is a major factor driving the evolution and ecology of microorganisms in many, if not all, environments.

Resource competition between microbes with overlapping niches can resolve in multiple ways, one of which relies on the production of anticompetitor compounds (i.e. compounds that directly inhibit ecological competitors) including bacteriocins (Riley & Wertz 2002a; Riley & Wertz 2002b). Anticompetitor strategies are highly advantageous because they increase resource availability for the producer (Kerr 2007). Bacteriocins are diverse, evolutionarily unrelated, toxic proteins and protein complexes produced by bacteria that often target strains and species closely related to the producer (Riley & Wertz 2002b; Michel-Briand & Baysse 2002). As such, they are recognized as effective anticompetitor compounds. Indeed, numerous empirical and theoretical studies have demonstrated the adaptive advantage of bacteriocin production (e.g. (Bakkal et al. 2010; Heo et al. 2007; Waite & Curtis 2009; Kerr et al. 2002)). In addition to basic scientific interest, there is considerable interest in harnessing and modifying bacteriocins as next generation pathogen control compounds (Gillor et al. 2004; Gillor et al. 2005; Cotter et al. 2005; Ritchie et al. 2011). Bacteriophage-derived bacteriocins (such as the R- and F-type pyocins) are of particular interest because of their ability to be reprogrammed to specifically target distantly related pathogens with few predicted side-effects (Ritchie et al. 2011).

While there has been considerable focus on the bacteriocins produced by *Pseudomonas aeruginosa* (Michel-Briand & Baysse 2002), there has been far less investigation into bacteriocin production and ecological roles for other Pseudomonads. *Pseudomonas syringae* has served as a model species to understand many aspects of plant-microbe interactions, including the microbial ecology of aerial plant surfaces (termed the *phyllosphere*) as well as the molecular and genomic bases of pathogen-plant interactions (Hirano & Upper 2000; Lindow & Brandl 2003; O'Brien, Thakur, et al. 2011b; O'Brien, Desveaux, et al. 2011a; Abramovitch et al. 2006; Lindeberg et al. 2009). Furthermore, there is a growing appreciation for the role of the water cycle in *P. syringae* dispersal and survival (reviewed in (Morris et al. 2013)), demonstrating the importance of environmental niches in the life cycle of this species. Although environmental factors and adaptive traits important for disseminating via the water cycle remain relatively unexplored (except for the role of ice nucleation activity), the factors

governing and phenotypic traits important for survival in association with plants are much better understood. An important aspect of fitness in the leaf enviroment for *P. syringae* (and other plant-associated bacteria) is the ability to access and exploit favorable leaf anatomic locations (intercellular grooves, base of glandular trichomes) where water and nutrients are relatively abundant (Lindow & Brandl 2003; Schoenherr 2006). Such scarcity and distribution of resources drives competition among bacteria inhabiting the aerial surfaces of plants (termed phyllosphere) (Wilson & Lindow 1994a; Wilson & Lindow 1994b). For certain coinhabitants, coexistence is mediated through resource partitioning, where dissimilarity between the catabolic potential allows the organisms to exploit distinct nutrient pools (Wilson & Lindow 1994a). For coinhabitants with highly similar catabolic potential, however, resources are not effectively partitioned, and thus the microbes compete directly for the same niche leading to competitive exclusion. In these cases, as well as in similar situations where *P. syringae* likely competes for limited nutrients outside of the plant environment (such as in epilithic biofilms), we hypothesize that bacteriocins produced by this species will structure both evolutionary dynamics and community composition. Indeed bacteriocins have been predicted among the sequenced genomes of *P. syringae* (reviewed in (Baltrus et al. 2014; Grinter, Milner, et al. 2012a; Holtsmark et al. 2008; Parret & De Mot 2002), with some members being biologically characterized (Grinter, Roszak, et al. 2012b).

In this work, we set out to assess the totality of bacteriocin content from 18 genomes representing the phylogenetic breadth of *P. syringae*, as well as assess the killing activity spectra from these same strains. In attempting to link the genotype to phenotype in the model strain, *P. syringae* B728a, we discovered its killing activity could not be explained by any predicted bacteriocins. In searching for the source of this killing activity, we have discovered a new bacteriophage-derived bacteriocin. This killing compound represents striking genomic and molecular convergence with a bacteriophage-derived bacteriocin of *P. aeruginosa* (R-type pyocin) but is independently derived. Additionally, we show that this phage-like bacteriocin region is largely conserved throughout *P. syringae*, and is present in other related *Pseudomonas* species, though its genomic location is variable. Thus, this killing compound is likely a major mediator of intraspecific interaction across this ecologically important genus.

Results

P. syringae strains commonly exhibit killing activity

Mitomycin C induction resulted in production of diverse killing patterns from *P. syringae* pvs. in culture supernatants, as evidenced by a zones of inhibition created by filtered supernatants in a lawn of target strains. The killing activity could be the result of a toxic compound or an activated prophage, which are commonly predicted in sequenced *P. syringae* genomes and have been recovered using this protocol (e.g. (Nordeen et al. 1983; Haag & Vidaver 1974)). The vast majority of clearing activity was not phage-mediated (Fig. 1). While we observed abundant bacteriocin-mediated clearing, we can't rule out the possibility that bacteriophages were present, but were not detected because their

activity was masked by the bacteriocins. *Ptt* exhibited the broadest-spectrum activity, killing 14 (78%) of test strains, respectively. *Pto* DC3K, *Pmp*, *Pan*, and *Pph* 1448a didn't produce killing activity against any strains tested. *Psy* B728a was unique among all of the strains tested, in that it displayed both phage-mediated and non-phage-mediated activity against *Pan*. In general, there was greater variance in the activity ranges between strains than there was in the sensitivity ranges between strains. Activity ranged between 0% and 70%, while sensitivity ranged between 10% and 45%. Certain distantly related strains exhibited largely similar (though not identical) killing spectra, including *Pto* T1, *Pla* 106, Cit7, *Pta*, and *Por* 1_6. Phylogroups I, II, and III are all represented approximately equally (5, 5, and 6 members, respectively), with members from recognized subgroups for phylogroups I and II represented (Berge et al. 2014), indicating that our results are not a product of sampling bias.

DNase-active bacteriocins are the most commonly predicted in P. syringae genomes

The genomes of all strains were analyzed using several approaches (see methods). Class III bacteriocins (> 10 kDa) with DNase catalytic domains (i.e. colicin E9, pyocin S3, and carocin D) were commonly predicted among the strains (Table 1). 13 of the 19 strains harbored one copy of a DNase-active bacteriocin, while *Psy* B728a and *Pmo* harbored two copies. Interestingly, several strains encode several immunity proteins (IPs) that would provide protection against the DNAase-active bacteriocins. *Pmp*, *Pan*, encode two DNase-IP copies (but only encode a single DNase killing protein), while *Pla*107 and *Pta* both encode three DNase-IP copies (but only encode a single DNase killing protein). Other colicin-like bacteriocins predicted include colicin E3-like (rRNase-active), colicin D-like (tRNase-active), and colicin M-like (Lipid I and II degrading [inhibition of cell wall synthesis]). The latter colicin-like bacteriocins were predicted in a minority of strains, often only in a single strain (Table 1). Interestingly, colicin M-like killing proteins were predicted in *Pla* 106, *Pto* DC3K, *Pmp*, and *Pja*, while no M-like IP was predicted in any of these strains. The colicin M predicted by us corresponds to that which was recently characterized (Grinter, Roszak, et al. 2012b). In addition to the colicin-like bacteriocins, putadicin-like bacteriocins (also class III) were predicted in multiple strains, including *Pmp*, *Ptt*, and *Pae*. Prediction of the putadicin-like bacteriocin in *Ptt* was previously reported (Ghequire et al. 2012). In addition to class III bacteriocins, there were several class I and II, collectively referred to as ribosomally-synthesized and post-translationally-modified peptides (RiPPs) predicted among the pathovars in this study, including microcin-like, lasso peptide-like, sactipeptide-like, and linear azol(in)e-containing peptide-like peptides and associated modification and transport proteins. The BAGEL2 and BAGEL3 databases used for bacteriocin prediction contain criteria for all major bacteriocin classes except for bacteriophage-derived bacteriocins, such as the R- and F-type pyocins produced by *Pseudomonas aeruginosa* (de Jong et al. 2010; van Heel et al. 2013).

Deletion of the predicted DNase-active colicin-like bacteriocins in P. syringae B728a results in no loss of killing activity against Pan, Pmp, Pae, Pph, and Pgy

We sought to confirm the genetic basis of the killing activity produced by *Psy* B728a. To this end, we constructed targeted gene deletions for the two predicted colicin-like bacteriocins, Psyr_0310 and Psyr_4651 (hereafter referred to as s-type syringacins after the naming convention established for *P. syringae* and *P. aeruginosa* (Michel-Briand & Baysse 2002; Grinter, Roszak, et al. 2012b)). Both s-type syringacins encode putatively DNase-active proteins. Deletion of Psyr_0310 and Psyr_4651, individually or in tandem, resulted in no detectable loss of killing activity against any strain targeted by the wild type *Psy* B728a (Fig. 2). This result indicated that the killing activity produced by *P. syringae* B728a is derived from a source not predicted by genome mining nor blastp queries with conserved catalytic domains.

P. syringae B728a harbors a prophage-like region, which is located in a syntenic region with the R and F-type pyocins encoded by Pseudomonas aeruginosa, that is responsible for its killing activity

The above results indicated that another locus (or loci) was responsible for the observed killing activity from *Psy* B728a. As the killing activity produced by this strain was more abundant from cultures treated with mitomycin C, we looked for the presence of RecA-mediated autopeptidase regulators, which are known to regulate bacteriocin production in *P. aeruginosa* and are mitomycin C responsive (Matsui et al. 1993). There are 9 open reading frames predicted in the Psy B728a genome that exhibit significant similarity to the consensus sequence for COG1974 (SOS-response transcriptional repressors) retrieved from the NCBI Conserved Domain Database (CDD) (Marchler-Bauer et al. 2013). One of the predicted RecA-mediated autopeptidases was found associated with the previously described prophage region II (Feil et al. 2005), which is syntenic to that of the R- and F-type pyocins (specifically between *trpE* and *trpG*) of *P. aeruginosa* PAO1 (Fig. 3). As both the R- and F-type pyocins are derived from bacteriophages (Nakayama et al. 2000), we hypothesized that prophage region II was responsible for the mitomycin C inducible killing activity. We constructed a series of deletion in both structural and regulatory genes associated with prophage region II (see Table S1 and Fig. S1). Deletion of a putative transcriptional regulator (Psyr_4603), encoding a RecA-mediated autopeptidase) as well as the promoter of a divergently transcribed hypothetical protein (Psyr_4602) resulted in loss of killing activity against all strains sensitive to *Psy* B728a (Fig. 2). Complementation by introduction of Psyr_4603 and Psyr_4602 (as well as flanking genomic sequence) in trans resulted in restored killing activity against all strains tested. Deletion of a region encompassing Psyr_4585 through Psyr_4592, which includes genes encoding structural components of baseplate, spike, and tail fiber, and tape measure (ΔR_{struct}), resulted in abolished killing activity against all strains. Deletion of the predicted receptor binding protein (Psyr_4585) and chaperone (Psyr_4584) that assists in attachment of the receptor binding protein to the bacteriophage tail (ΔR_{rbp}), also resulted in abolished killing activity against all strains. Expression of Psyr_4585/Psyr_4584

from a constitutive promoter in trans resulted in restored killing activity against all strains. It should be noted, complementation was only possible for constructs which included an upstream alternative start codon (Fig. S2). Taken together, the genetic and phenotypic data convincingly demonstrate the bacteriophage-derived region is responsible for the intraspecific killing activity produced by *Psy* B728a. In keeping with nomenclature for *P. aeruginosa*, we refer to the killing complex produced by *P. syringae* as an R-type syringacin.

The R-type syringacin of P. syringae is derived from an independent bacteriophage, and thus represents evolutionary convergence with the R-type pyocin at genomic, molecular, and phenotypic levels

Despite the conserved synteny between the R-type pyocin and R-type syringacin, very few genes in these regions exhibit similarity detectable using a blastp search with low stringency (E-value cut off $\leq 10^{-5}$) (Fig. 3). The R-type syringacin of *Psy* B728a was originally described as being related to a Mu-like bacteriophage based on gene content and arrangement (Feil et al. 2005). To further confirm that the R-type syringacin is not derived from the same progenitor of the R-type pyocin of *P. aeruginosa*, we compared the gene content between *trpG* and *trpE* across multiple Pseudomonads (Fig. 4A). Across the *Pseudomonas* phylogeny (as described in (Loper et al. 2012)), the gene content between *trpE* and *trpG* is variable. Importantly, the R-type syringacin region located between *trpE* and *trpG* is only found in the *P. syringae* clade; the other Pseudomonads closely related to *P. syringae* including *Pseudomonas putida*, *Pseudomonas flurosescens*, and *Pseudomonas chlororaphis* do not harbor any predicted prophage or prophage-like elements in this region. The most parsimonious explanation for these results is that the R-type syringacin was integrated in the progenitor of the *P. syringae* lineage and is independent of the R-type pyocin.

Additionally, a nucleotide alignment of the sequences surrounding and including the R-type pyocin and syringacin regions demonstrated high nucleotide sequence identity between the two strains for *trpE* and *trpG* (including genes operonic with these loci), but negligible nucleotide identity corresponding to the regions encoding the respective R-type bacteriocins (Fig 3). This result corresponds well with the poor amino acid similarity between the ORFs of these regions: those genes located in the *trpE* and *trpG* operons are well conserved at the amino acid level between the two strains, while very few genes within the respective bacteriocin regions have detectable amino acid sequence similarity, and those that do exhibit relatively little similarity (Fig. 3).

To further confirm that the R-type syringacin from *P. syringae* is derived independently of the R-type pyocin from *P. aeruginosa*, we performed phylogenetic reconstructions using a maximum likelihood-based (ML) approach for three proteins where amino acid similarity could be detected by blastp across *P. syringae* B728a, *P. aeruginosa* PAO1, phage Mu, and phage P2 using a transitive homology approach (Roessler et al. 2008). Based on the functions predicted or described for the orthologs from P2 and Mu (Morgan et al. 2002; Leiman & Shneider 2012), Psyr_4587 encodes a component of the baseplate,

Psyr_4589 encodes the spike, and Psyr_4595 encodes the tail sheath protein. For all proteins, there was overwhelming support that the orthologs from *P. syringae* B728a (as well as all other *P. syringae* strains examined in this study, except for those where the protein was truncated [see below]) were more closely related to those from phage Mu (96-100 bootstrap support), while the orthologs from *P. aeruginosa* were more closely related to those from phage P2 (92-100 bootstrap support; Figs. 5, S3, and S4). Thus, the phylogenetic inference supports the R-type syringacin being derived from an independent bacteriophage (a Mu-like bacteriophage) rather than the R-type pyocin, despite both R-type bacteriocins being located in a syntenic genomic region. These results are similar to those reported previously, where Mavrodi et al. 2009 found the R-type syringacin region (therein reported as genomic island 12) from *P. syringae* B278a exhibited nucleotide similarity to prophage 1 of *P. protegens* (*P. fluorescens*) Pf-5, while the R-type pyocin of *P. aerugionas* PAO1 exhibited nucleotide similarity to prophage 3 of Pf-5.

While our analyses indicate the R-type syringacin has been derived independently of the R-type pyocin, comparing the gene content of the R-type syringacin to phage Mu, demonstrates the loss and retention of similar genes to that described for the R-type pyocin. Specifically, the R-type syringacin lacks all genes corresponding to the early and middle region of the phage Mu genome (encoding functions related to phage replication). The genes retained that correspond to the late region of phage Mu, are only those related to tail morphogenesis, while late genes related to capsid morphogenesis and DNA packaging have been lost (Fig. 6). This pattern of gene retention mirrors that of the R-type pyocin when compared to phage P2 (Nakayama et al. 2000). These results indicate convergent bacteriophage domestication at both genomic and phenotypic levels, likely resulting from similar evolutionary and ecological pressures.

The R-type syringacin is conserved across Pseudomonas with loss of R-type genes in P. syringae associated with lack of detectable killing activity

While the gene content between *trpE* and *trpG* across the *Pseudomonas* strains presented in figure 4A indicated that only *P. syringae* and *P. aeruginosa* harbor R-type bacteriocins, a previous report (Mavrodi et al. 2009) demonstrated nucleotide conservation between prophage 1 of *P. fluorescens* Pf-5 (recently renamed to *P. protegens* Pf-5, (Ramette et al. 2011)) and the R-type syringacin (referred to as genomic island 12). We confirmed the homology of these regions by comparing the amino acid conservation and synteny of genes in their respective regions (Fig. 7 and Table S2). There is significant similarity at the amino acid level between most of the tail structural genes. Additionally, the order of genes is syntenic between the two organisms. The most dissimilar proteins between the two regions are those encoding the receptor binding proteins (also referred to as the tail fibers), Psyr_4585 and PFL_1226, exhibiting only 66% amino acid similarity over 8.6% of the length of Psyr_4585). This result is not unexpected, however, given this protein's role in host recognition, and that it is a highly divergent protein between related bacteriophages (Veesler & Cambillau

2011). Our results in conjunction with those previously reported, indicate that prophage I of *P. protegens* Pf-5 is homologous to the R-type syringacin, and thus likely encodes a killing compound within this organism.

As previously shown (Loper et al. 2012; Mavrodi et al. 2009) prophage I of *P. protegens* Pf-5 is similar to prophage regions found in closely related *P. fluorescens* strains as well as other Pseudomonads. These previous results indicate that R-type syringacin-like elements exist in *P. chlororaphis* 30-84, *P. chlororaphis* O6, and *P. fluorsecens* PfO-1. Inspecting the genomes of all strains shown in figure 4 using blastp with several R-type syringacin genes used as the queries, further demonstrated R-type syringacin regions present in *P. brassicacearum* NFM421, *P. entimophila* L48, *P. putida* S16, and *P. putida* KT2440 (Fig 4B).

Phylogenetic analysis of this region, using concatenated homologs of Psyr_4587, Psyr_4589, and Psyr_4595, across these strains indicates largely, but not entirely, vertical inheritance (Fig. 8). Clustering of *P. entomophila* with *P. fluorescens*, *P. brassicacearum*, and *P. chlororaphis*, instead of with the *P. putida* strains, to which *P. entomophila* is more closely related, for all individual protein phylogenies (Figs. S5-S7) as well as the concatenated phylogeny (Fig. 8) is well supported (bootstrap values ≥ 70). The most parsimonious explanation for this result is gain of R-type syringacin by *P. entomophila* from the ancestor of the *P. fluorescens* clade. The placement of *P. syringae* UB246 is inconsistent among the phylogenies. *P. syringae* UB246 is an early diverging strain of this species (Morris et al. 2010; Berge et al. 2014). The concatenated phylogeny (with poor bootstrap support) as well as the phylogeny of Psyr_4595 orthologs (with strong bootstrap support) indicate the *P. syringae* UB246 R-type syringacin is more closely related to the R-type regions from *P. putida*, than it is to the R-type regions of the other *P. syringae* strains. The single gene phylogenies for Psyr_4587 and Psyr_4589 place the *P. syringae* UB246 ortholog on a branch including, and sister to, all of the strains except *P. putida* strains, or outside of all the *Pseudomonas* species, including *P. putida*, respectively. Taken together, the exact relationship of the R-type syringacin of *P. syringae* UB246 to the other R-type regions will depend on further sampling.

Comparison of this region across the *P. syringae* strains phenotypically characterized in this study revealed broad conservation (Table 2). In looking at conservation across *P. syringae* pathovars, we have observed the trend that strains with no killing activity detected in this study (*Pto* DC3K, *Pmp*, *Pan*, *Pph* 1448A) are all missing numerous genes associated with the R-type syringacin, including genes demonstrated to necessary for acitivity in *Psy* B728a.

Renaming of genes associated with the R-type syringacin

As we have described the function and a portion of the molecular determinants for a bacteriophage derived bacteriocin in *P. syringae* B728a, we have renamed genes associated with this complex to *rtsA-J* for R-type syringacin (see table 2)

Discussion

Given the diversity and distribution of bacteriocins across *P. syringae*, as well as related Pseudomonads (Loper et al. 2012; Parret & De Mot 2002), it is highly likely that these systems mediate ecological and evolutionary interactions between organisms in the plant environment and beyond. Indeed, that Mavrodi et al. found the region harboring the R-type bacteriocin present in *P. fluorescens* strain Q8r1-96 but absent in strain Q2-87, which is less competent at colonizing the wheat rhizosphere, indicates that this region could affect root colonization (Mavrodi et al. 2009; Mavrodi et al. 2002). Additionally, Garrett et al. found a general trend where *P. syringae* isolates recovered from citrus tended to produce bacteriocins active against isolates recovered from pear and vice versa (Garrett et al. 1966). Direct demonstration of the benefit of bacteriocins in plant colonization is still lacking, and thus is an area ripe for future investigation.

Previous work by Fischer et al. demonstrated the presence of a bacteriophage tail-like bacteriocin produced by *P. fluorescens* SF4c, which killed related *P. fluorescens* strains (Fischer et al. 2012). Comparing the results of Fischer et al. with Loper et al., the phage-tail bacteriocin of SF4c is related to the prophage I in Pf0-1, as described in (Loper et al. 2012). In Pf0-1, this region is located immediately upstream of prophage II, which is related to the R-type syringacin described in this study. Thus, it appears that bacteriophage-derived bacteriocins are more common and widespread throughout *Pseudomonas* than previously recognized. Both this work and previous work found R-type syringacin-like regions throughout the *Pseudomonas* intragenic cluster II (Yamamoto et al. 2000), including *P. protegens*, *P. chlororaphis*, *P. fluorescens*, *P. brassicacearum*, *P. putida*, *P. entomophila*, and *P. syringae* (Loper et al. 2012; Mavrodi et al. 2009). While the R-type syringacin is widely distributed through out this group of related Pseudomonads, its evolutionary history is complex. This region appears after the divergence of *P. aeruginosa* from other species. In *P. syringae*, the R-type region is found nearly exclusively between *trpE* and *trpG*, the only exception being strain UB246, an early diverging member of *P. syringae sensu lato* (Berge et al. 2014), indicating a single introduction into this species. Supporting the conclusion of a single introduction into *P. syringae*, in all phylogenies, the UB246 orthologs are sister to all other *P. syringae* proteins, likely indicating the introduction occurred prior to the diversification of this species. Within the *P. fluorescens*/*P. chloroaphis*/*P. protegens* clade, the R-type region appears to be ancestral as it is located in a single genomic region, and is lost by *P. fluorescens* strains SBW25 and A506, which constitute a monphyletic clade (with 100 bootstrap support as reported in (Loper et al. 2012), Fig. 4). The pattern of retention in *P. putida*/*P. entomophila*, however, is more complex. Several strains of *P. putida* do not contain the R-type syringacin region (strains W619, GB-1, F1, BIRD-1), while strains S16 and KT2440 do contain this region, though in different genomic locations. Additionally, despite *P. entomophila* being more closely related to *P. putida*, all phylogenetic analyses supported its R-type region being more closely related to that from *P. fluorescens*/*P. chloroaphis*/*P. protegens*. Thus, in addition to the intragenomic mobility of this region, there appears to be intergenomic mobility as well.

The results presented above clearly demonstrate the domestication of a retractile-type bacteriophage into a retractile-type bacteriocin independent of the R-type pyocin of *Pseudomonas aeruginosa*. At the DNA level, there is a high degree of identity between *P. aeruginosa* and *P. syringae* in the *trpE* and *trpG* (and surrounding genomic regions) that is absent within the corresponding bacteriocin regions. Additionally, amino acid sequence similarity between the genes associated with each bacteriocin is scant, and likely reflects similarity based on conserved function, as both bacteriocins are derived from related bacteriophages (both in the *myoviridae* family) (Leiman & Shneider 2012). Finally, the phylogenetic reconstruction based on three structural proteins, all provided strong support for separating all of the *P. syringae* R-type syringacin sequences into a monophyletic clade with bacteriophage Mu, while all of *P. aeruginosa* R-type pyocin sequences were present in a monophyletic clade with bacteriophage P2, thus indicating they are independently derived.

The convergence between these two bacteriocins is striking at both the genomic and molecular levels. The most parsimonius explanation for the distribution of the R-type syringacin region is that it integrated into the *trpE* and *trpG* region following domestication (i.e. not as an active prophage). It is currently unclear what features favor mobilization into this region. In any event, the convergence of these events implies there is selective pressure for genetic integration at this locus in *Pseudomonas*. At the molecular level, there is a similar profile of gene retention and loss between the R-type pyocin and R-type syringacin. Gene encoding functions related to replication, capsid morphogenesis, and DNA packaging have been lost in the domesticated bacteriocins, with only genes encoding functions related to the bacteriophage tail morphogenesis being retained. Again these results point to a strong selective pressure favoring the domestication of bacteriophages into killing complexes. This result is analogous to that of the domesticated endogenous viral elements (EVEs) of the parisitoid wasps, where there are at least two independent domestication events leading to complexes aiding in the parasitoid lifestyle in separate wasp families (Braconidae and Ichneumonidae) (Herniou et al. 2013). We hypothesize that such viral domestications play an important role in the evolution and diversification of species.

Materials and Methods

Plasmids, primers, bacterial isolates, and growth conditions

All bacterial strains and plasmids are listed in table S6. All primers are listed in table S7. *P. syringae* were routinely grown at 27°C on King's medium B (KB) (King et al. 1954). *E. coli* was routinely grown in lysogeny broth (LB) (Bertani 1951) at 37°C. When appropriate, growth media was supplemented with antibiotics or sugars at the following concentrations: 10 µg/ml tetracycline, 50 µg/ml kanamycin, 25 µg/ml gentamycin, 50 µg/ml rifampicin, nitrofurantoin (NFT) 50 µg/ml, and 5% (w/v) sucrose.

Deletion and complementation of bacteriocin loci

Colicin-like and R-type-associated syringocin loci were deleted using an overlap-extension approach similar to that described in (Hockett et al. 2014). Approximately 0.8-1.0 kilobase pairs flanking targeted genes were amplified using *Pfx* polymerase (a proof reading polymerase). Amplified fragments were separated and purified from an agarose gel using the QIAquick Gel Extraction Kit (Qiagen, Valencia, CA) and combined into a subsequent PCR. Combined fragments (in the absence of primers) were cycled 10x, after which BP tailing primer R and F were added and allowed to 20 additional cycles. The desired product was isolated from an agarose gel and combined with the entry vector (pDONR207) in a BP clonase reaction (Invitrogen, Carlsbad, CA). Gentamycin resistant colonies were screened using PCR to confirm the presence of desired DNA fragment. Entry vectors confirmed to harbor the correct fragments were combined with the destination vector (pMTN1907) in an LR clonase reaction (Invitrogen). Following this reaction, kanamycin resistant colonies were screened using PCR, one colony confirmed to contain the correct fragment was used as the mating donor in a tri-parental conjugation with *P. syringae* B728a and DAB44 (mating helper). Matings were plated on KB amended with rifampacin, NFT, and tetracycline. Colonies were screened by PCR to harbor the desired construct. A single confirmed isolate was incubated over night in unamended KB, afterwhich it the resultant culture was serially diluted and spotted onto KB amended with sucrose (counter selection against integrated pMTN1907). Single colonies were picked and confirmed to retain the desired deletion by PCR, as well as to be tetracycline sensitive.

For complementation, genes or operons containing their native promoters were amplified using *Pfx*. Amplified fragments were tailed with BP primers in a subsequent PCR and cloned into pDONR207 in a BP clonase reaction. Isolates confirmed by PCR to contain the desired fragment served as the donor vectors in an LR clonase reaction with either pJC531 (R_{reg}) or pBAV226 (R_{rbp}) as the destination vector. Plasmid was isolated from one isolate harboring the destination vector confirmed to contain the desired fragment, which was subsequently electroporated into the appropriate *P. syringae* B728a deletion mutant.

Assay for killing activity

Bacteriocin production was induced by treating log-phase broth cultures with mitomycin C (mitC, 0.5 ng/ml, final concentration), which were allowed to incubate for an additional 12 to 24 hours. Supernatant from induced cultures was collected by centrifuging surviving cells and cell debris and was sterilized either by filtration using a 0.2 µm filter or by adding 5-10 µl of chloroform to culture supernatant. Bacteriocins were occasionally concentrated to increase detectable killing activity using polyethylene glycol (PEG) precipitation. PEG precipitation was performed by adding NaCl (1.0 M final concentration) and PEG 8000 (10% final concentration) to culture supernatants and either incubated in an ice water bath for 1 hour or at 4 °C over night. Samples were centrifuged at 16k G for 30 minutes at 4 °C. Supernatants were decanted and samples were resuspended in

1/10 or 1/100 original volumne in buffer (0.01 M Tris, 0.01 M $MgSO_4$, pH 7.0). Residual PEG was removed by extracting twice with equal columes of chloroform. Sterile supernatants (concentrated or not) were tested for killing activity using a standard agar overlay technique (Grinter, Roszak, et al. 2012b). Briefly, 100 µl of log phase broth tester culture was combined with 3 ml molten soft-agar (0.4% agar) which was mixed by vortexing and poured over a standard KB agar plate (1.5% agar). Plates were allowed to solidify for 30 minutes to 1 hour prior to spotting 5 µl of mitC induced, sterilized supernatant. Plates were allowed to incubate for 24-48 hours after which the presence or absence of a clearing zone was determined. To differentiate between bacteriocin-derived clearing and bacteriophage-derived clearing, two tests were performed. First, serial 1/5 dilutions were plated onto the same tester strain. If killing activity was derived from a bacteriophage, dilutions were found where the clearing zone resolved into distinct plaques, while killing activity from a bacteriocin did not. Second, material from zones of clearing on a bacterial lawn was transferred using a sterile tooth-pick to a subsequent agar overlay plate of the same tester strain. Clearing zones derived from bacteriophages yielded clearing on the subsequent plate, while clearing zones derived from bacteriocins did not yield subsequent clearing.

Non-R-type bacteriocin prediction and genomic comparison

Colicin-like bacteriocins and their associated immunity proteins (IPs) were predicted by using characterized catalytic domains and IPs (provided by D. Walker, University of Glasgow) as queries using blastp. Additionally, the recently described lectin-like bacteriocin (Ghequire et al. 2012) served as a query using blastp. Pathovar genomes were analyzed using both BAGEL2 and BAGEL3 web-based programs (de Jong et al. 2010; van Heel et al. 2013), which predicts a number of different types of bacteriocins, including class I, II, and III bacteriocins. Bacteriocin prediction using BAGEL3 was not performed until after completion of the R-type bacteriocin, thus, the carocin D-like bacteriocin in *Psy* B728a was not targeted for deletion as the source of the killing activity had already been determined.

R-type bacteriocin prediction and genomic comparison

The genomic region immediately surrounding *trpE* and *trpG* was aligned between *P. syringae* B728a and *P. aeruginosa* PAO1 using progressive Mauve (implemented in Geneious v6.1.8, created by Biomatters, available from http://www.geneious.com/). Additionally, genes were compared between the two strains at the amino acid level using blastp. Hits exhibiting and E-value of 10^{-5} or less were considered significant.

The gene content of the R-type bacteriocins of *P. syringae* B728a and *P. aeruginosa* PAO1 were compared to phage Mu and phage P2, respectively, at the amino acid level using blastp. Hits exhibiting and E-value of 10^{-5} or less were considered significant.

Gene content across the *Pseudomonas* genus was compared using the gene ortholog neighborhood viewer (based on best bidirectional blast hit) at the Integrated Microbial Genomes (IMG) website (https://img.jgi.doe.gov/) with both

trpE and *trpG* as queries. Comparison of R-type syringacin gene content across *P. syringae* pathovars was also performed using the gene ortholog neighborhood viewer (best bidirectional blast hit). Additionally, genes within the R-type syringacin region that are bacteriophage derived were compared across pathovars using blastp.

Phylogenetic inference of selected genes

We used a transitive homology approach (Roessler et al. 2008) to identify proteins that exhibited detectable amino acid similarity across the R-type bacteriocin regions from *P. syringage* B728a and *P. aeruginosa* PAO1, as well as from phages Mu and P2. Three proteins were recoverd, including Psyr_4587 (corresponding to gp47 [Mu], gpJ [P2], and PA0618 [*P. aeruginosa*]), Psyr_4589 (corresponding to gp45 [Mu], gpV [P2], and PA0616 [*P. aeruginosa*]), and Psyr_4595 (corresponding to gp39 [Mu], gpFI [P2], and PA0622 [*P. aeruginosa*]). Using blastp searches, homologs representing a range of percent identity with Psyr_4587, Psyr_4589, and Psyr_4595 were collected from the NCBI-nr database, as well from all bacteriophage, *P. syringae*, and *P. aeruginosa* genomes available in the IMG database. Truncated and duplicate (in terms of amino acid identity) sequences were excluded from phylogenetic analyses. Hits were aligned with the MAFFT v1.3.3 plug-in (Katoh & Standley 2013) in Geneious v6.1.5 (Biomatters Ltd.) using L-INS-i under Blosum30, with a gap open penalty of 1.53 and an offset value of 0.123.

Maximum-likelihood (ML) heuristic searches were used to estimate phylogenies with RAxML v8.0.9 on the CIPRES Science Gateway under either the WAG + I + G (Psyr_4587, PA0618, gp47, and gpJ), WAG + I + G (Psyr_4589, PA0616, gp45, and gpV), WAG + G + F (Psyr_4595, PA0622, gpL, and gpFI), LG + G + F (Concatenation of multiple sequence alignments for Psyr_4587, Psyr_4589, and Psyr_4595 homologs from *Pseudomonas*), WAG + G (Psyr_4587 and homologs from *Pseudomonas*), LG + G (Psyr_4589 and homologs from *Pseudomonas*), or LG + G + F (Psyr_4595 and homologs from *Pseudomonas*), WAG + I + G + F (gp45 homologs), WAG + G + F (gp47 homologs, or WAG + G + F (L_Psyr homologs), models of evolution as determined by the Bayesian Information Criterion in ProtTest v3.2 (Abascal et al. 2005). Searches for the phylogenetic reconstruction with the highest likelihood score were performed simultaneously with 1000 rapid bootstrapping replicates. Resulting phylogenies were edited with FigTree v1.3.1 (http://tree.bio.ed.ac.uk/software/figtree/) and Adobe Illustrator.

Acknowledgements

Support for K.L.H provided by startup funds to D.A.B from the University of Arizona, School of Plant Sciences. T.R. acknowledges support from the National Institutes of Health (K12 GM000708). We thank Erick Karlsrud, Kevin Dougherty, and Rachel Murillo for their help in generating and testing of various mutants presented in this work. We thank Daniel Walker for supplying bacteriocin catalytic domain sequences.

References

Abascal, F., Zardoya, R. & Posada, D., 2005. ProtTest: selection of best-fit models of protein evolution. *Bioinformatics*, 21(9), pp.2104–2105.

Abramovitch, R.B., Anderson, J.C. & Martin, G.B., 2006. Bacterial elicitation and evasion of plant innate immunity. *Nature Reviews: Molecular Cell Biology*, 7(8), pp.601–611.

Almeida, N.F. et al., 2008. A Draft Genome Sequence of Pseudomonas syringae pv. tomato T1 Reveals a Type III Effector Repertoire Significantly Divergent from That of Pseudomonas syringae pv. tomato DC3000. *Molecular plant-microbe interactions : MPMI*, 22(1), pp.52–62.

Arnison, P.G. et al., 2012. Ribosomally synthesized and post-translationally modified peptide natural products: overview and recommendations for a universal nomenclature. *Natural product reports*, 30(1), pp.108–160.

Bakkal, S. et al., 2010. Role of bacteriocins in mediating interactions of bacterial isolates taken from cystic fibrosis patients. *Microbiology*, 156(7), pp.2058–2067.

Baltrus, D.A. et al., 2011. Dynamic Evolution of Pathogenicity Revealed by Sequencing and Comparative Genomics of 19 Pseudomonas syringae Isolates. *Plos Pathogens*, 7(7).

Baltrus, D.A. et al., 2012. The Molecular Basis of Host Specialization in Bean Pathovars of Pseudomonas syringae. *Molecular plant-microbe interactions : MPMI*, 25(7), pp.877–888.

Baltrus, D.A., Hendry, T.A. & Hockett, K.L., 2014. Ecological Genomics of Pseudomonas syringae. In D. C. Gross, A. Lichens-Park, & C. Kole, eds. *Genomics of Plant-Associated Bacteria*. Springer Berlin Heidelberg, pp. 59–77.

Berge, O. et al., 2014. A User's Guide to a Data Base of the Diversity of Pseudomonas syringae and Its Application to Classifying Strains in This Phylogenetic Complex. *PloS one*, 9(9), pp.–e105547.

Bertani, G., 1951. Studies on Lysogenesis .1. the Mode of Phage Liberation by Lysogenic Escherichia-Coli. *Journal of bacteriology*, 62(3), pp.293–300.

Buell, C.R. et al., 2003. The complete genome sequence of the Arabidopsis and tomato pathogen Pseudomonas syringae pv. tomato DC3000. *Proceedings of the National Academy of Sciences*, 100(18), pp.10181–10186.

Chang, J.H. et al., 2005. A high-throughput, near-saturating screen for type III effector genes from Pseudomonas syringae. *Proceedings of the National Academy of Sciences of the United States of America*, 102(7), pp.2549–2554.

Cotter, P.D., Hill, C. & Ross, R.P., 2005. Bacteriocins: developing innate immunity for food. *Nature Reviews Microbiology*, 3(10), pp.777–788.

de Jong, A. et al., 2010. BAGEL2: mining for bacteriocins in genomic data. *Nucleic Acids Research*, 38(suppl 2), pp.W647–W651.

Demoling, F., Figueroa, D. & Bååth, E., 2007. Comparison of factors limiting bacterial growth in different soils. *Soil Biology and Biochemistry*, 39(10), pp.2485–2495.

Ditta, G. et al., 1980. Broad Host Range Dna Cloning System for Gram-Negative Bacteria - Construction of a Gene Bank of Rhizobium-Meliloti. *Proceedings of the National Academy of*

Sciences of the United States of America, 77(12), pp.7347–7351.

D'Argenio, D., 2004. The Pathogenic Lifestyle of Pseudomonas aeruginosa in Model Systems of Virulence. In J.-L. Ramos, ed. *Pseudomonas*. Boston, MA: Springer US, pp. 477–503–401.

Farrer, R.A. et al., 2009. De novo assembly of the Pseudomonas syringae pv. syringae B728a genome using Illumina/Solexa short sequence reads. *FEMS Microbiology Letters*, 291(1), pp.103–111.

Feil, H. et al., 2005. Comparison of the complete genome sequences of Pseudomonas syringae pv. syringae B728a and pv. tomato DC3000. *Proceedings of the National Academy of Sciences of the United States of America*, 102(31), pp.11064–11069.

Fischer, S. et al., 2012. Characterization of a phage-like pyocin from the plant growth-promoting rhizobacterium Pseudomonas fluorescens SF4c. *Microbiology*, 158(Pt 6), pp.1493–1503.

Garrett, C.M.E., Panagopoulos, C.G. & Crosse, J.E., 1966. Comparison of Plant Pathogenic Pseudomonads From Fruit Trees. *Journal of Applied Bacteriology*, 29(2), pp.342–&.

Ghequire, M.G.K. et al., 2012. Plant lectin-like antibacterial proteins from phytopathogens Pseudomonas syringae and Xanthomonas citri. *Environmental Microbiology Reports*, 4(4), pp.373–380.

Gillor, O., Kirkup, B.C. & Riley, M.A., 2004. Colicins and Microcins: The Next Generation Antimicrobials A2 . In *Advances in Applied Microbiology*. Advances in Applied Microbiology. Academic Press, pp. 129–146 T2 –.

Gillor, O., Nigro, L.M. & Riley, M.A., 2005. Genetically engineered bacteriocins and their potential as the next generation of antimicrobials. *Current Pharmaceutical Design*, 11(8), pp.1067–1075.

Grinter, R., Milner, J. & Walker, D., 2012a. Bacteriocins active against plant pathogenic bacteria. *Biochemical Society Transactions*, 40(6), pp.1498–1502.

Grinter, R., Roszak, A.W., et al., 2012b. The Crystal Structure of the Lipid II-degrading Bacteriocin Syringacin M Suggests Unexpected Evolutionary Relationships between Colicin M-like Bacteriocins. *Journal of Biological Chemistry*, 287(46), pp.38876–38888.

Haag, W.L. & Vidaver, A.K., 1974. Purification and characterization of syringacin 4-A, a bacteriocin from pseudomonas syringae 4-A. *Antimicrobial Agents and Chemotherapy*, 6(1), pp.76–83.

Harrison, F., 2007. Microbial ecology of the cystic fibrosis lung. *Microbiology*, 153(4), pp.917–923.

Heo, Y.-J. et al., 2007. R-Type pyocin is required for competitive growth advantage between Pseudomonas aeruginosa strains. *Journal of Microbiology and Biotechnology*, 17(1), pp.180–185.

Herniou, E.A. et al., 2013. When parasitic wasps hijacked viruses: genomic and functional evolution of polydnaviruses. *Philosophical Transactions of the Royal Society B: Biological Sciences*, 368(1626), pp.20130051–20130051.

Hirano, S.S. & Upper, C.D., 2000. Bacteria in the Leaf Ecosystem with Emphasis onPseudomonas syringae—a Pathogen, Ice Nucleus, and Epiphyte. *Microbiology and Molecular Biology Reviews*, 64(3), pp.624–653.

Hockett, K.L. et al., 2014. Pseudomonas syringae CC1557: A Highly Virulent Strain With an Unusually Small Type III Effector Repertoire That Includes a Novel Effector. *Molecular plant-microbe interactions : MPMI*, 27(9), pp.923–932.

Holtsmark, I., Eijsink, V.G.H. & Brurberg, M.B., 2008. Bacteriocins from plant pathogenic bacteria. *FEMS Microbiology Letters*, 280(1), pp.1–7.

Joardar, V. et al., 2005. Whole-Genome Sequence Analysis of Pseudomonas syringae pv. phaseolicola 1448A Reveals Divergence among Pathovars in Genes Involved in Virulence and Transposition. *Journal of bacteriology*, 187(18), pp.6488–6498.

Katoh, K. & Standley, D.M., 2013. MAFFT Multiple Sequence Alignment Software Version 7: Improvements in Performance and Usability. *Molecular Biology and Evolution*, 30(4), pp.772–780.

Kerr, B., 2007. The Ecological and Evolutionary Dynamics of Model Bacteriocin Communities. In M. Riley & M. Chavan, eds. *Bacteriocins*. Berlin, Heidelberg: Springer Berlin Heidelberg, pp. 111–134–134.

Kerr, B. et al., 2002. Local dispersal promotes biodiversity in a real-life game of rock-paper-scissors. *Nature*, 418(6894), pp.171–174.

King, E.O., Ward, M.K. & Raney, D.E., 1954. Two simple media for the demonstration of pyocyanin and fluorescin. *Journal of Laboratory and Clinical Medicine*, 44, pp.301–307.

Leiman, P.G.P. & Shneider, M.M.M., 2012. Contractile tail machines of bacteriophages. In M. G. Rossmann & V. B. Rao, eds. *Advances in Experimental Medicine and Biology*. Advances in Experimental Medicine and Biology. Boston, MA: Springer US, pp. 93–114–114. Available at: http://eutils.ncbi.nlm.nih.gov/entrez/eutils/elink.fcgi?dbfrom=pubmed&id=22297511&retmode=ref&cmd=prlinks.

Lindeberg, M., Cunnac, S. & Collmer, A., 2009. The evolution of Pseudomonas syringae host specificity and type III effector repertoires. *Molecular Plant Pathology*, 10(6), pp.767–775.

Lindow, S.E. & Brandl, M.T., 2003. Microbiology of the Phyllosphere. *Applied and environmental microbiology*, 69(4), pp.1875–1883.

Loper, J.E. et al., 2012. Comparative genomics of plant-associated Pseudomonas spp.: insights into diversity and inheritance of traits involved in multitrophic interactions. *PLoS genetics*, 8(7), p.e1002784.

Lugtenberg, B. & Kamilova, F., 2009. Plant-Growth-Promoting Rhizobacteria. *Annual Review of Microbiology*, 63(1), pp.541–556.

Lugtenberg, B.J.J. & Bloemberg, G.V., 2004. Life in the Rhizosphere. In J.-L. Ramos, ed. *Pseudomonas*. Boston, MA: Springer US, pp. 403–430–430.

Marchler-Bauer, A. et al., 2013. CDD: conserved domains and protein three-dimensional structure. *Nucleic Acids Research*, 41(Database issue), pp.D348–52.

Matsui, H. et al., 1993. Regulation of pyocin genes in Pseudomonas aeruginosa by positive (prtN) and negative (prtR) regulatory genes. *Journal of bacteriology*, 175(5), pp.1257–1263.

Mavrodi, D.V. et al., 2002. Identification of differences in genome content among phlD-positive Pseudomonas fluorescens strains by using PCR-based subtractive hybridization. *Applied*

and environmental microbiology, 68(10), pp.5170–5176.

Mavrodi, D.V. et al., 2009. Mobile genetic elements in the genome of the beneficial rhizobacterium Pseudomonas fluorescens Pf-5. *BMC Microbiology*, 9(1), p.8.

Michel-Briand, Y. & Baysse, C., 2002. The pyocins of Pseudomonas aeruginosa. *Biochimie*, 84(5–6), pp.499–510.

Morgan, G.J. et al., 2002. Bacteriophage Mu genome sequence: analysis and comparison with Mu-like prophages in Haemophilus, Neisseria and Deinococcus. *Journal of Molecular Biology*, 317(3), pp.337–359.

Morris, C.E. et al., 2010. Inferring the Evolutionary History of the Plant Pathogen Pseudomonas syringae from Its Biogeography in Headwaters of Rivers in North America, Europe, and New Zealand. *Mbio*, 1(3), pp.–.

Morris, C.E. et al., 2008. The life history of the plant pathogen Pseudomonas syringae is linked to the water cycle. *Isme Journal*, 2(3), pp.321–334.

Morris, C.E., Monteil, C.L. & Berge, O., 2013. The Life History of Pseudomonas syringae: Linking Agriculture to Earth System Processes. *Annual Review of Phytopathology, Vol 51*, 51, pp.85–104.

Nakayama, K. et al., 2000. The R-type pyocin of Pseudomonas aeruginosa is related to P2 phage, and the F-type is related to lambda phage. *Molecular Microbiology*, 38(2), pp.213–231.

Nordeen, R.O., Morgan, M.K. & Currier, T.C., 1983. Isolation and Partial Characterization of Bacteriophages of the Phytopathogen Pseudomonas syringae. *Applied and environmental microbiology*, 45(6), pp.1890–1898.

O'Brien, H.E., Desveaux, D. & Guttman, D.S., 2011a. Next-generation genomics of Pseudomonas syringae. *Current Opinion in Microbiology*, 14(1), pp.7–7.

O'Brien, H.E., Thakur, S. & Guttman, D.S., 2011b. Evolution of plant pathogenesis in Pseudomonas syringae: a genomics perspective. *Annual Review of Phytopathology, Vol 51*, 49(1), pp.269–289.

Parret, A. & De Mot, R., 2002. Bacteria killing their own kind: novel bacteriocins of pseudomonas and other gamma-proteobacteria. *Trends in Microbiology*, 10(3), pp.107–112.

Ramette, A. et al., 2011. Pseudomonas protegens sp. nov., widespread plant-protecting bacteria producing the biocontrol compounds 2,4-diacetylphloroglucinol and pyoluteorin. *Systematic and Applied Microbiology*, 34(3), pp.180–188.

Riley, M.A. & Wertz, J.E., 2002a. Bacteriocin diversity: ecological and evolutionary perspectives. *Biochimie*, 84(5–6), pp.357–364.

Riley, M.A. & Wertz, J.E., 2002b. BACTERIOCINS: Evolution, Ecology, and Application. *Annual Review of Microbiology*, 56(1), pp.117–137.

Ritchie, J.M. et al., 2011. An Escherichia coli O157-Specific Engineered Pyocin Prevents and Ameliorates Infection by E. coli O157:H7 in an Animal Model of Diarrheal Disease. *Antimicrobial Agents and Chemotherapy*, 55(12), pp.5469–5474.

Roessler, C.G. et al., 2008. Transitive homology-guided structural studies lead to discovery of

Cro proteins with 40% sequence identity but different folds. *Proceedings of the National Academy of Sciences*, 105(7), pp.2343–2348.

Schoenherr, J., 2006. Characterization of aqueous pores in plant cuticles and permeation of ionic solutes. *Journal of Experimental Botany*, 57(11), pp.2471–2491.

Sørensen, J. & Nybroe, O., 2004. Pseudomonas in the Soil Environment. In J.-L. Ramos, ed. *Pseudomonas*. Boston, MA: Springer US, pp. 369–401.

van Heel, A.J. et al., 2013. BAGEL3: automated identification of genes encoding bacteriocins and (non-)bactericidal posttranslationally modified peptides. *Nucleic Acids Research*, 41(W1), pp.W448–W453.

Veesler, D. & Cambillau, C., 2011. A Common Evolutionary Origin for Tailed-Bacteriophage Functional Modules and Bacterial Machineries. *Microbiology and Molecular Biology Reviews*, 75(3), pp.423–433.

Vinatzer, B.A. et al., 2006. The type III effector repertoire of Pseudomonas syringae pv. syringae B728a and its role in survival and disease on host and non-host plants. *Molecular Microbiology*, 62(1), pp.26–44.

Waite, R.D. & Curtis, M.A., 2009. Pseudomonas aeruginosa PAO1 Pyocin Production Affects Population Dynamics within Mixed-Culture Biofilms. *Journal of bacteriology*, 191(4), pp.1349–1354.

Wilson, M. & Lindow, S.E., 1994a. Coexistence among Epiphytic Bacterial Populations Mediated through Nutritional Resource Partitioning. *Applied and environmental microbiology*, 60(12), pp.4468–4477.

Wilson, M. & Lindow, S.E., 1994b. Ecological Similarity and Coexistence of Epiphytic Ice-Nucleating (Ice(+)) Pseudomonas-Syringae Strains and a Non-Ice-Nucleating (Ice(-)) Biological-Control Agent. *Applied and environmental microbiology*, 60(9), pp.3128–3137.

Yamamoto, S. et al., 2000. Phylogeny of the genus Pseudomonas: intrageneric structure reconstructed from the nucleotide sequences of gyrB and rpoD genes. *Microbiology*, 146(10), pp.2385–2394.

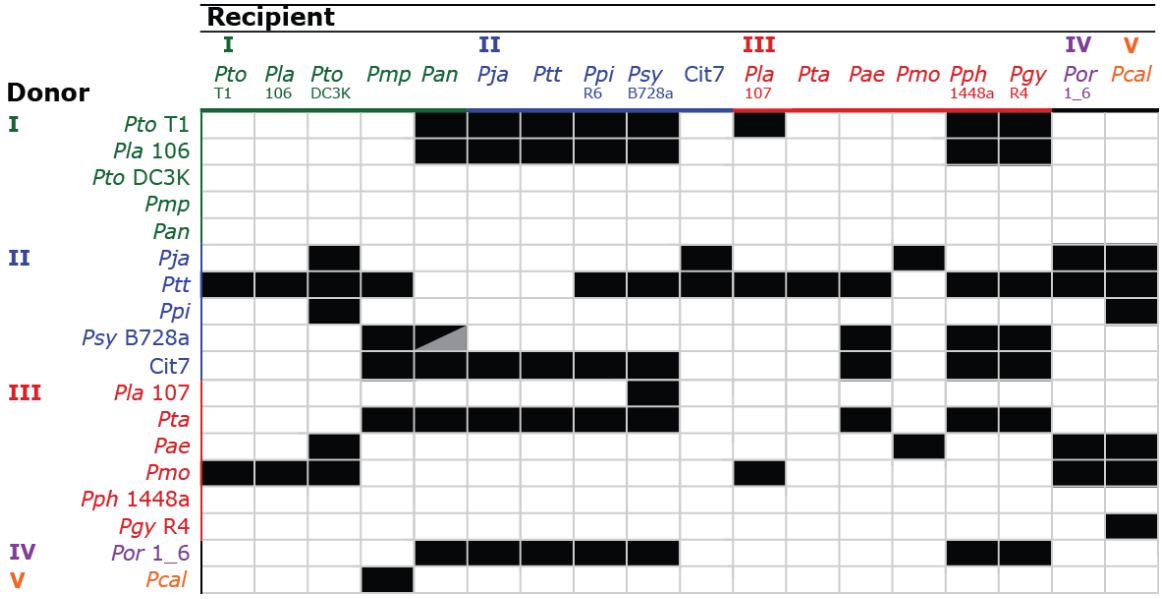

Figure 1. Killing activities of *P. syringae* pathovars. Rows indicate the source of killing activity. Columns target of killing activity. Activities are as follows: no killing activity detected (white box), non-bacteriophage-mediated killing activity (black box), and bacteriophage-mediated killing activity (gray box). Color coded according to clades in (Baltrus et al. 2011).

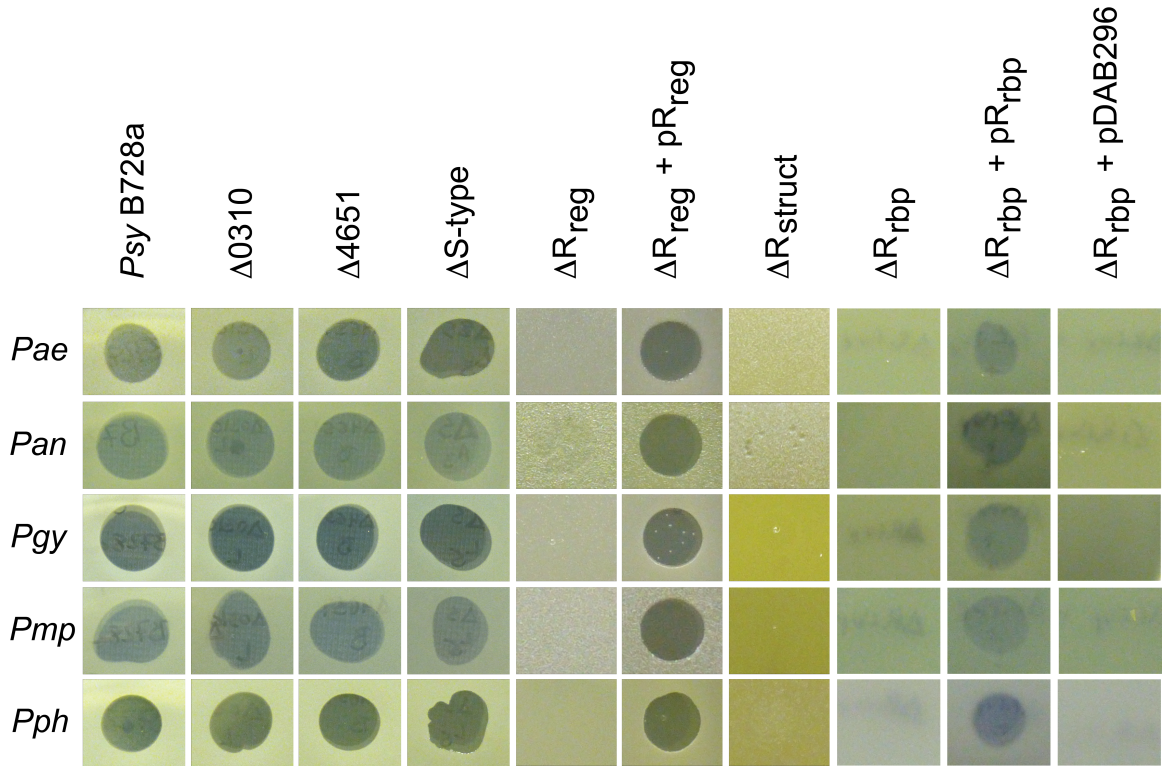

Figure 2. Clearing activity produced by *Psy* B728a and various bacteriocin deletion mutants against select pathovars. 2-5 µl of filter-sterilized, mitC induced culture supernatant was spotted onto soft agar overlays of the indicated pathovars (rows). *Psy* B728a (wild type); Δ0310 (deletion of Psyr_0310); Δ4651 (deletion of Psyr_4651); ΔS-type (deletion of both Psyr_0310 and Psyr_4651); ΔR_{reg} (deletion of Psyr_4603 promoter and coding sequence, deletion of Psyr_4602 promoter); ΔR_{reg} + pR_{reg} (R_{reg} deletion with both Psyr_4603 and Psyr_4602, as well as surrounding genomic sequence, complemented *in trans* on a replicative vector); $\Delta R_{struct.}$ (deletion of Psyr_4592 through Psyr_4586, as well as the promoter of Psyr_4585); ΔR_{rbp} (deletion of Psyr_4584 and Psyr_4585); ΔR_{rbp} + pR_{rbp} (Psyr_4584 and Psyr_4585 expressed from a constitutive promoter in pBAV226); ΔR_{rbp} + pDAB296 (pBAV266 empty vector).

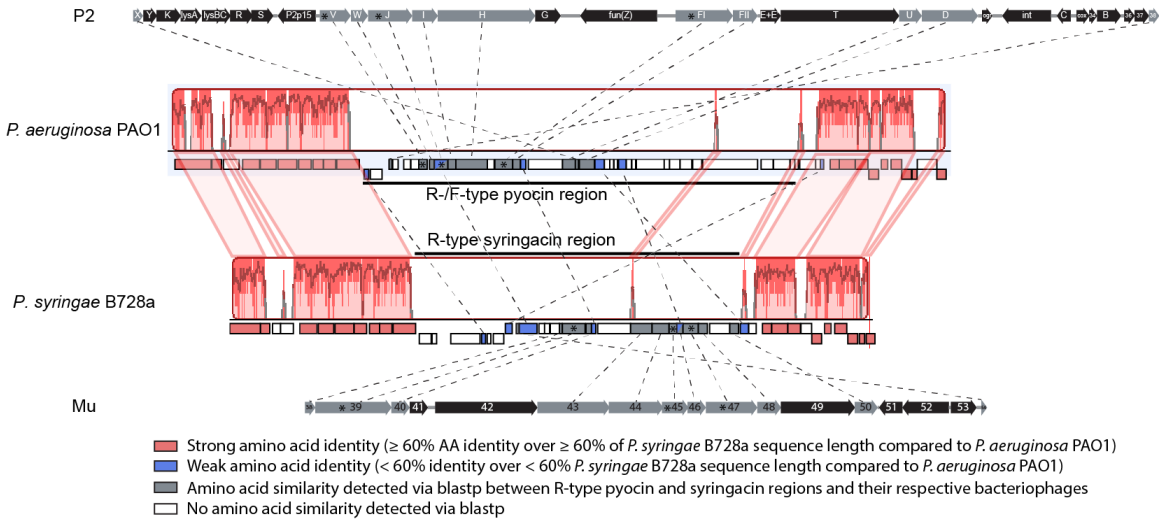

Figure 3. Comparison of genomic regions flanked by *trpE* and *trpG* between *P. syringae* B728a and *P. aeruginosa* PAO1. Regions between *P. aeruginosa* PAO1 and *P. syringae* B728a connected pink shading indicate regions of significant nucleotide identity as assessed by progressive Mauve. Dashed lines were omitted between conserved genes in regions of nucleotide identity between *P. aeruginosa* PAO1 and *P. syringae* B728a, however gene synteny between the two strains is conserved. Dashed lines between bacterial and bacteriophage genomes indicate genes exhibiting amino acid similarity detectable by blastp. Genes marked by asterisks indicate those utilized for the phylogenetic analyses.

Figure 4. Comparison of gene content between *trpE* and *trpG* (A) or between *mutS* and *cinA* (B) across select *Pseudomonas* species. Phylogeny is adapted from (Loper et al. 2012) which was constructed using maximum likelihood based 726 proteins shared across the genomes. Genes and genomic regions are colored as follows: conserved genes demarcating the genomic location (gray arrows), non-phage related genes (black arrows), R-type syringacin-like region (red), R- and F-type pyocin-like regions (blue), prophage I region described in (Loper et al. 2012) (green), undescribed prophage regions (black).
**P. putida* KT2440 contains an R-type syringocin region, but not in either of the noted genomic locations.

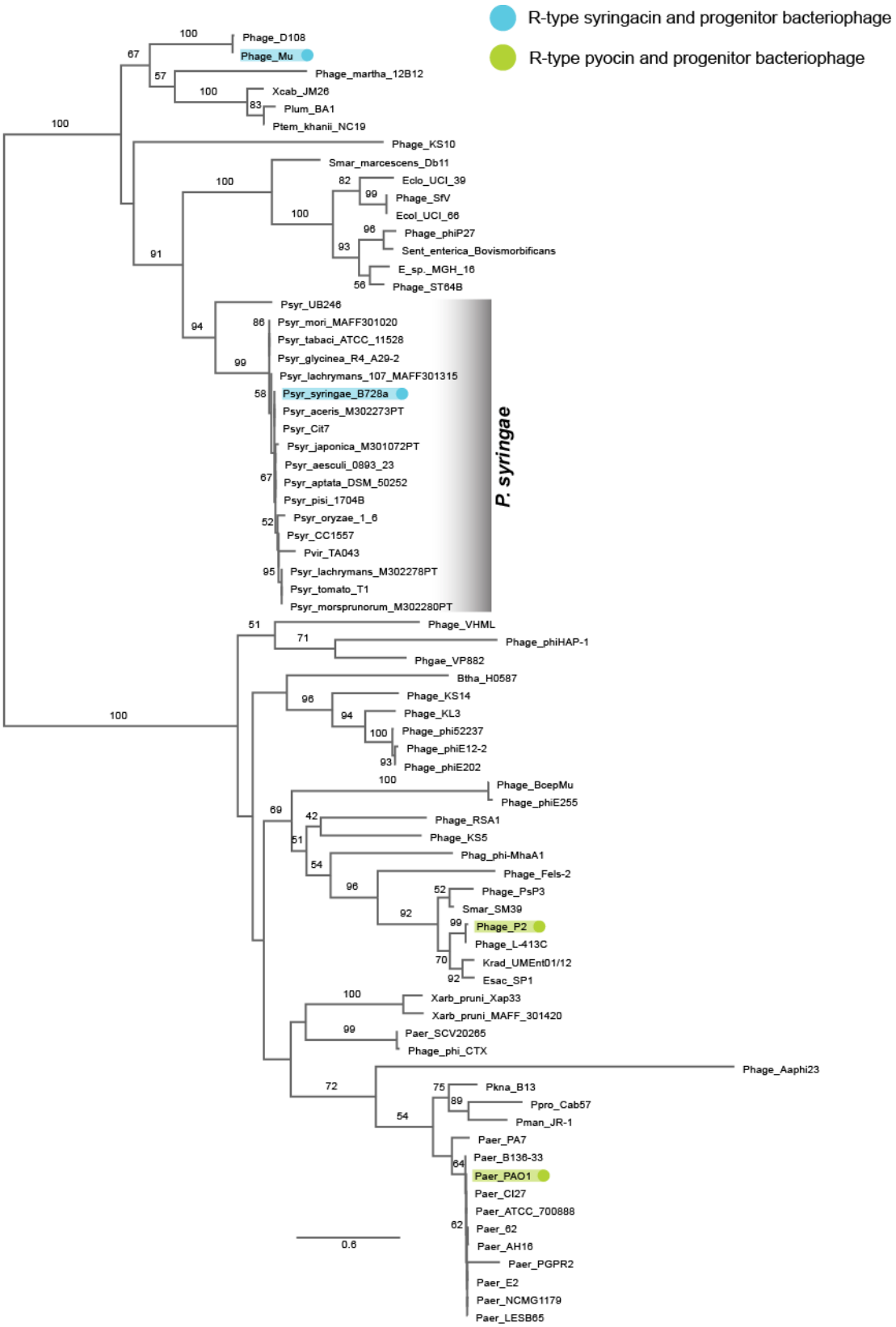

Figure 5. Maximum likelihood phylogeny of Psyr_4589 (*P. syringae* B728a), PA0616 (*P. aeruginosa* PAO1), gp45 (Mu), and gpV (P2) and related protein sequences from bacteria and bacteriophages. Teal highlighted nodes indicate Psyr_4589 and gp45, while green highlighted

nodes indicate PA0616 and gpV. Values on branches indicate bootstrap support (1000 bootstrap replicates) for those clades (only values of 50 or greater are shown). A monophyletic clade including all *P. syringae* orthologs is indicated. See table S4 for accessions or IMG GeneIDs associated with each sequence.

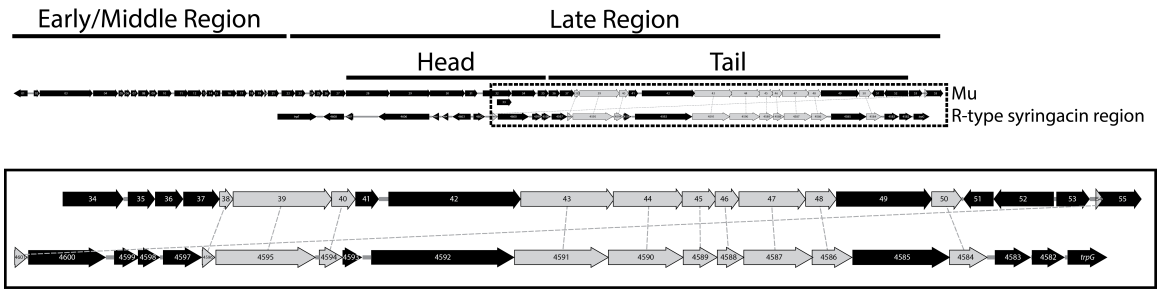

Figure 6. Comparison of gene content in R-type syringocin region and bacteriophage Mu genome. Genes exhibiting detectable amino acid similarity by blastp are indidcated in gray. Designation of phage Mu gene categories (early, middle, late, head, tail) taken from (Morgan et al. 2002).

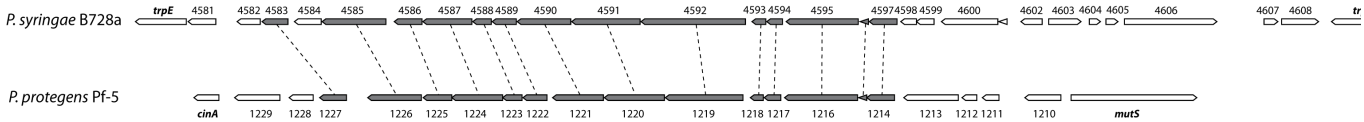

Figure 7. Comparison of gene content between the R-type syringacin of *P. syringae* B728a and prophage I of *P. protegens* Pf-5. Genes with gray shading indicate significant blastp similarity. Unshaded genes indicate no amino acid similarity detectable by blastp. *trpE* and *trpG* indicate the boundary of the R-type syringacin region, while *cinA* and *mutS* indicate the boundary of prophage I. See table S2 for a % amino acid similarity and identity between homologous genes. Genes and intergenic regions are drawn to scale.

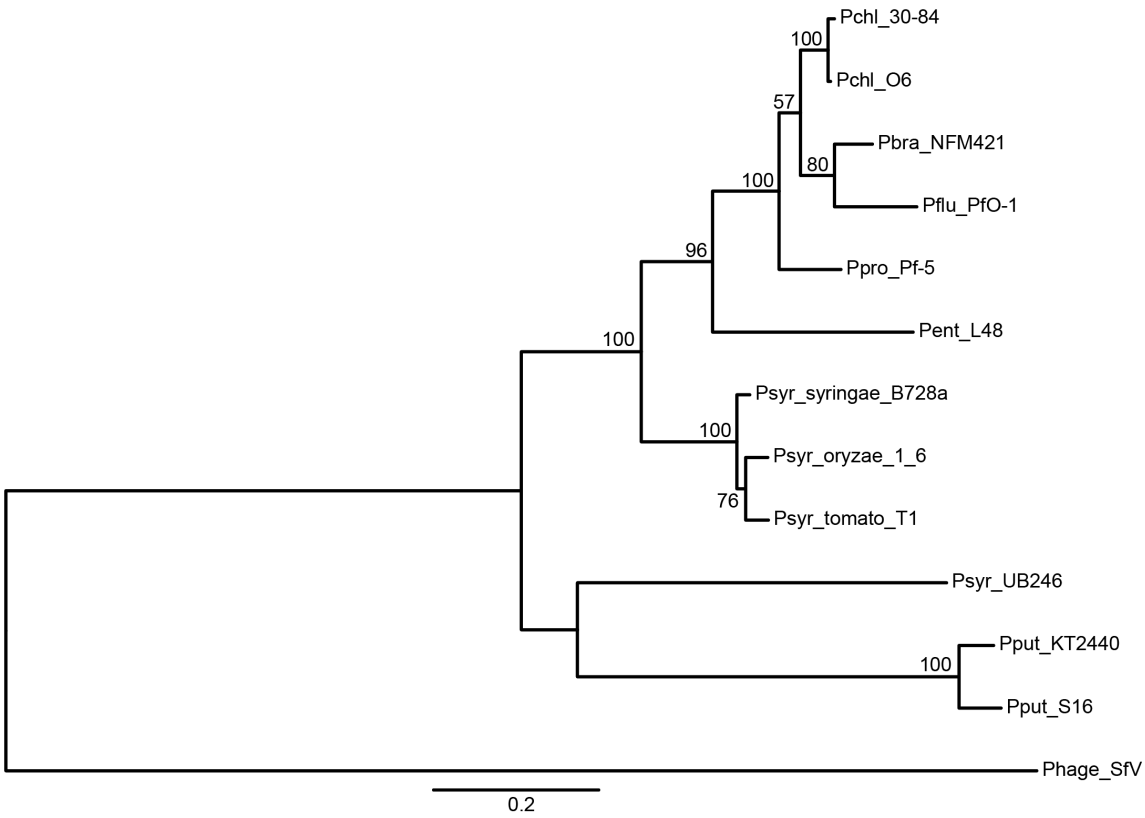

Figure 8. Maximum likelihood phylogeny of concatenated amino acid sequences of Psyr_4587, Psyr_4589, and Psyr_4595, and their homologs from *Pseudomonas* strains harboring an R-type syringocin-like region. Values indicate bootstrap support (out of 1000 replicates, only values greater than 50 are shown). The following strains are Pchl 30-84 (*P. chlororaphis* 30-84), Pchl O6 (*P. chlororaphis* O6), Pbra NFM421 (*P. brasicacearum* NFM421), Pflu PfO-1 (*P. fluorescens* PfO-1), Ppro Pf-5 (*P. protegens* Pf-5), Pent L48 (*P. entomophila* L48), Psyr B728a (*P. syringae* pv. syringae B728a), Psyr 1_6 (*P. syringae* pv. oryzae 1_6), Psyr T1 (*P. syringae* pv. tomato T1), Psyr UB246 (*P. syringae* UB246), Pput KT2440 (*P. putida* KT2440), Pput S16 (*P. putida* S16). Phage SfV (bacteriophage SfV, outgroup).

	Class III (>10 kDa) Bacteriocins													RiPPs			
	DNase						rRNase		tRNase		PG inhibiting						
	Col E9	IP	Pyo S3	IP	Car D	IP	Col E3	IP	Col D	IP	Col M	IP	Put like	Microcin like	Lasso peptide like	Sacti-peptide like	LAP[a] like
Pto T1	1	1	-	-	1	1	-	-	1	1	-	-	-	-	-	-	-
Pla 106	1	1	-	-	1	1	-	-	-	-	1	-	-	-	1	-	-
Pto DC3K	1	1	-	-	1	1	-	-	-	-	1	-	-	-	-	-	-
Pmp	1	2	-	-	1	1	1	-	-	-	1	-	1	-	1	-	-
Pan	1	2	-	-	-	-	-	-	-	-	-	-	-	-	-	-	-
Pja	-	1	-	-	-	-	-	-	-	-	1	-	-	-	1	-	-
Ptt	-	-	-	-	-	-	-	-	-	-	-	-	1	-	-	-	-
Ppi	-	-	-	-	1	1	-	-	-	-	-	-	-	-	-	-	-
Psy B728a	2	2	-	-	1	1	-	-	-	-	-	-	-	-	-	-	-
Cit7	1	1	-	-	1	1	-	-	-	-	-	-	-	1	1	-	-
Pla 107	1	3	-	-	-	-	-	-	-	-	-	-	-	1	-	1	-
Pta	1	3	-	-	1	1	-	-	-	-	-	-	-	2	-	-	-
Pae	-	-	-	-	-	-	-	-	-	-	-	-	1	3	1	-	1
Pmo	2	1	-	-	-	-	-	-	-	-	-	-	-	1	1	-	-
Pph 1448a	-	1	-	-	1	1	-	-	-	-	-	-	-	1	-	-	-
Pgy R4	1	1	-	-	1	1	-	-	-	-	-	-	-	1	1	-	-
Por 1_6	1	1	-	-	-	-	-	-	-	-	-	-	-	-	1	-	-
Pcal	1	1	-	1	-	-	-	-	-	-	-	-	-	1	-	-	-

Table 1: Bacteriocins predicted in *P. syringae* genomes. Predicted class III bacteriocins include colicin E9 (Col E9), pyocin S3 (Pyo S3), carocin D (Car D), colicin E3 (Col E3), colicin D (Col D), colicin M (Col M), and putadicin-like (Put like). Mode-of-action is noted for class III bacteriocins, including DNase, rRNase, tRNase, and peptidoglycan (PG) inhibiting. Additional class III bacteriocins that were searched for (based on catalytic domain similarity) but that were not predicted include colicins E5, A, B, E1, and N. Presence of cognate immunity proteins (IP) for each class III bacteriocin is indicated. Predicted class I and II bacteriocins (<10 kDa) are collectively referred to as ribosomally-synthesized and post-translationally-modified peptides (RiPPs) as described in (Arnison et al. 2012). Numbers indicate the number of distinct homologs in each genome.
[a]Linear azol(in)e-containing peptide

Table 2. Conservation of R-type syringacin across *P. syringae*.

Psyr #	Gene symbol	*Pto* T1	*Pla* 106	*Pto* DC3K	*Pmp*	*Pan*	*Pja*	*Ptt*	*Ppi* R6	Cit7	*Pla* 107	*Pta*	*Pae*	*Pmo*	*Pph*	*Pgy*	*Por* 1_6	*Pcal*	UB246
4584	*rtsP*																		47/63
4585	*rtsO*																		48/62
4586	*rtsN*																		64/76
4587	*rtsM*																		58/72
4588	*rtsL*																		48/67
4589	*rtsK*																		55/71
4590	*rtsJ*																		51/70
4591	*rtsI*																		44/63
4592	*rtsH*																		42/62
4593	*rtsG*																		54/70
4594	*rtsF*																		56/71
4595	*rtsE*																		62/75
4596	*rtsD*																		54/69
4601	*rtsC*	88/95	88/95	88/95			90/95	90/95	91/98							95/98	84/93		
4602	*rtsB*																		51/71
4603	*rtsA*																		29/43

50-74% ID
75-84% ID
85-94% ID
≥95% ID

*Cells colored in shades of red indicate gene presence with the noted % amino acid identity to the Psy B728a homolog, which are syntenic to the R-type syringacin in *Psy* B728a. Cells noted in gray are syntenic to the R-type syringacin of *Psy* B728a and exhibit amino acid similarity detectable by blastp, but have less than 60% query coverage (potentially indicating the gene is truncated compared to the ortholog in *Psy* B728a). Dark green cells indicate genes that exhibit significant amino acid identity and similarity (%identity/%similarity) to the noted gene in *Psy* B728a, however the genes are present in a non-syntenic region of the noted genome. Light green cells indicate genes that exhibit significant amino acid identity and similarity to the noted gene in *Psy* B728a, however their location within their respective genomes can't be determined. All of the genes noted in blue in UB246 exhibit detectable similarity those indicated in *Psy* B728a, additionally the genes are present in the same order as those in the R-type syringacin, however, they are located in a different genomic region (not flanked by *trpE* and *trpG*).

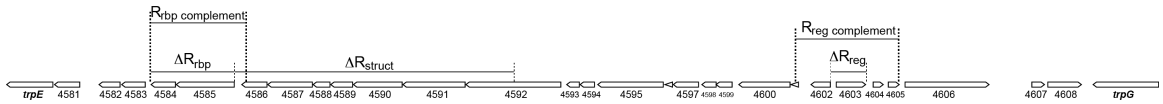

Figure S1. Map of R-type syringacin deletion and complementing constructs. Zones of deletion constructs (ΔR_{rbp}, ΔR_{struct}, and ΔR_{reg}) indicate regions removed in deletion strains. Zones of complement constructs (R_{rbp} complement and R_{reg} complement) indicate regions introduced on replicative plasmids (pBAV226 and pMTN41, respectively).

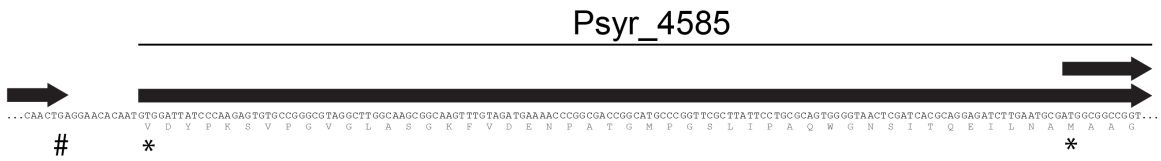

Figure S2. Original and updated annotated start codon for Psyr_4585. Right most * indicates original start codon (as annotated in (Feil et al. 2005) genome release, GOLD project ID: Gp0000484). Left most * indicates alternative upstream start codon (as annotated in (Farrer et al. 2009) genome release, GOLD project ID: Gp004223). Upstream # indicates the stop codon for Psyr_4586.

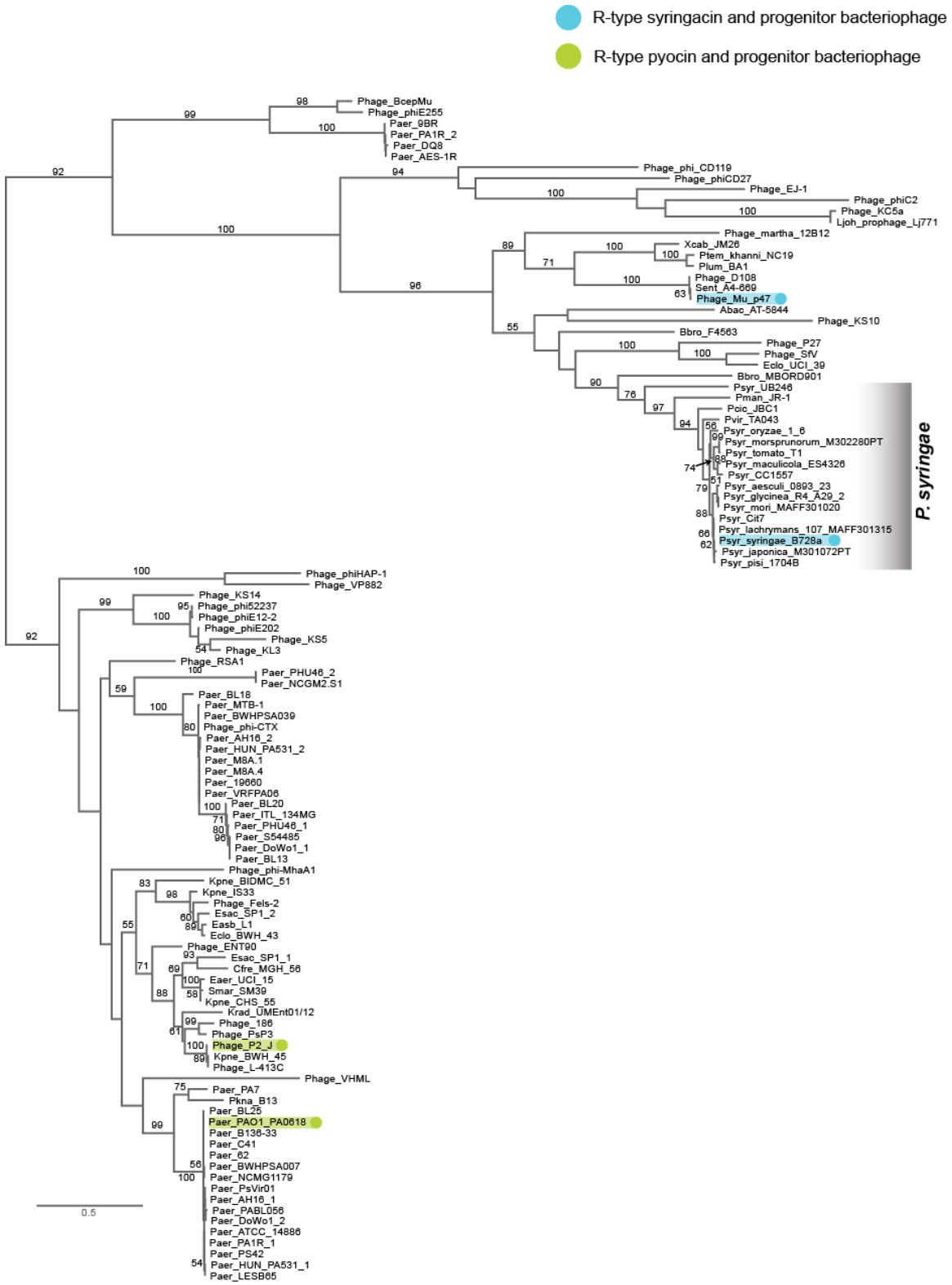

Figure S3. Maximum likelihood phylogeny of Psyr_4587 (*P. syringae* B728a), PA0618 (*P. aeruginosa* PAO1), gp47 (Mu), and gpJ (P2) and related protein sequences from bacteria and bacteriophages. Teal highlighted nodes indicate Psyr_4587 and gp47, while green highlighted

nodes indicate PA0618 and gpJ. Values on branches indicate bootstrap support (1000 bootstrap replicates) for those clades (only values of 50 or greater are shown). A monophyletic clade including all *P. syringae* orthologs is indicated. See table **S3** for accessions or IMG GeneIDs associated with each sequence.

Figure S4. Maximum likelihood phylogeny of Psyr_4595 (*P. syringae* B728a), PA0622 (*P. aeruginosa* PAO1), gpL (Mu), and gpFI (P2) and related protein sequences from bacteria and

bacteriophages. Teal highlighted nodes indicate Psyr_4595 and gpL, while green highlighted nodes indicate PA0622 and gpFI. Values on branches indicate bootstrap support (1000 bootstrap replicates) for those clades (only values of 50 or greater are shown). A monophyletic clade including all *P. syringae* orthologs is indicated. See table S5 for accessions or IMG GeneIDs associated with each sequence.

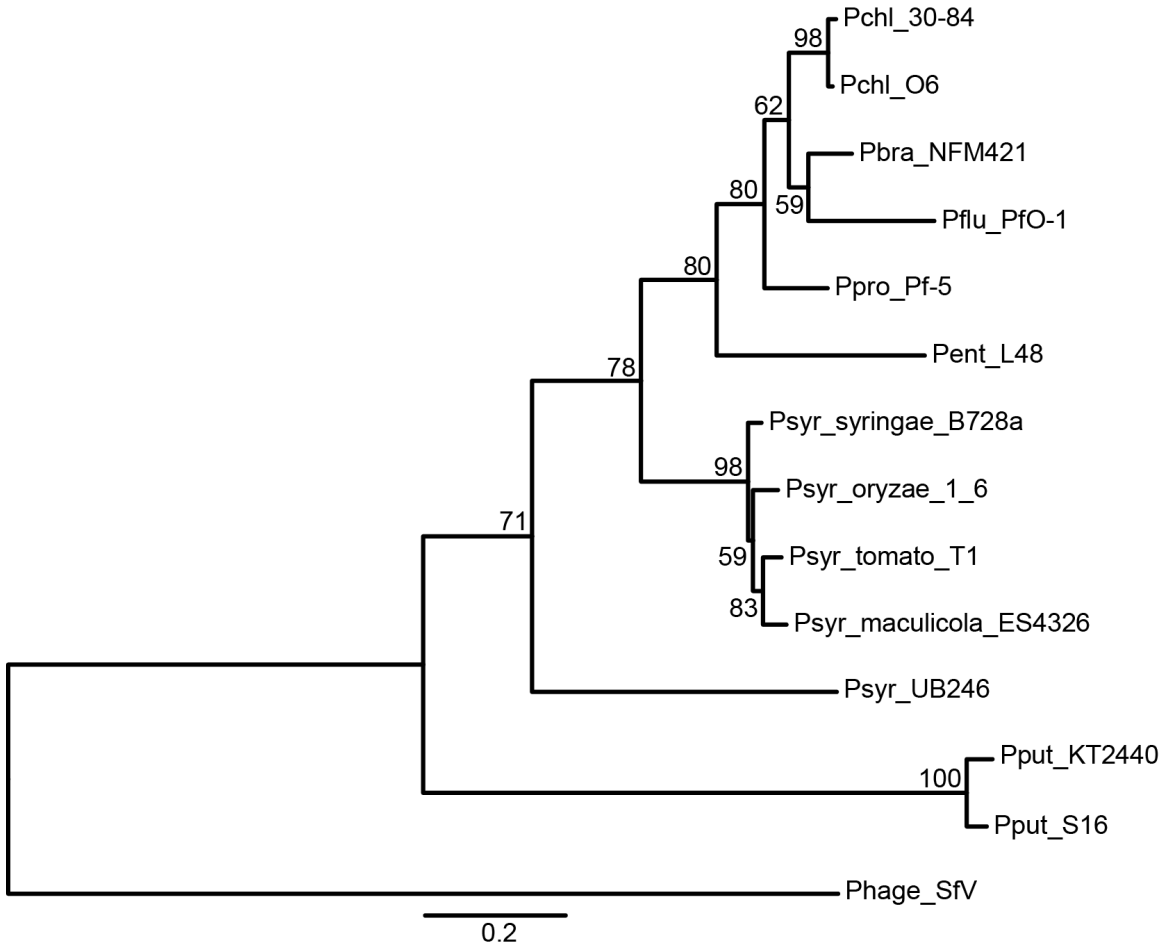

Figure S5. Maximum likelihood phylogeny of amino acid sequence of Psyr_4587 and its homologs from *Pseudomonas* strains harboring an R-type syringocin-like region. Values indicate bootstrap support (out of 1000 replicates, only values greater than 50 are shown). The following strains are Pchl 30-84 (*P. chlororaphis* 30-84), Pchl O6 (*P. chlororaphis* O6), Pbra NFM421 (*P. brasicacearum* NFM421), Pflu PfO-1 (*P. fluorescens* PfO-1), Ppro Pf-5 (*P. protegens* Pf-5), Pent L48 (*P. entomophila* L48), Psyr B728a (*P. syringae* pv. syringae B728a), Psyr 1_6 (*P. syringae* pv. oryzae 1_6), Psyr T1 (*P. syringae* pv. tomato T1), Pcan ES4326 (*P. cannabina* pv. alisalensis ES4326), Psyr UB246 (*P. syringae* UB246), Pput KT2440 (*P. putida* KT2440), Pput S16 (*P. putida* S16). Phage SfV (bacteriophage SfV, outgroup).

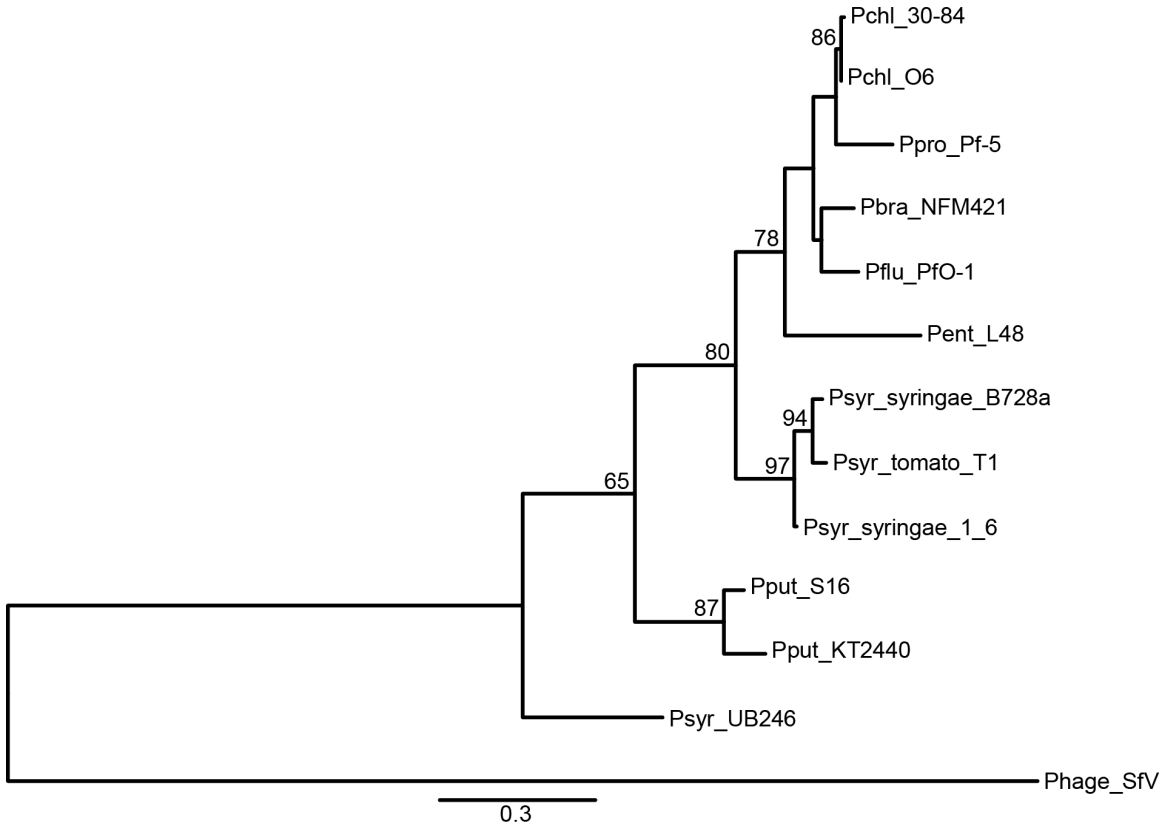

Figure S6. Maximum likelihood phylogeny of amino acid sequence of Psyr_4589 and its homologs from *Pseudomonas* strains harboring an R-type syringocin-like region. Values indicate bootstrap support (out of 1000 replicates, only values greater than 50 are shown). The following strains are Pchl 30-84 (*P. chlororaphis* 30-84), Pchl O6 (*P. chlororaphis* O6), Pbra NFM421 (*P. brasicacearum* NFM421), Pflu PfO-1 (*P. fluorescens* PfO-1), Ppro Pf-5 (*P. protegens* Pf-5), Pent L48 (*P. entomophila* L48), Psyr B728a (*P. syringae* pv. syringae B728a), Psyr 1_6 (*P. syringae* pv. oryzae 1_6), Psyr T1 (*P. syringae* pv. tomato T1), Pcan ES4326 (*P. cannabina* pv. alisalensis ES4326), Psyr UB246 (*P. syringae* UB246), Pput KT2440 (*P. putida* KT2440), Pput S16 (*P. putida* S16). Phage SfV (bacteriophage SfV, outgroup).

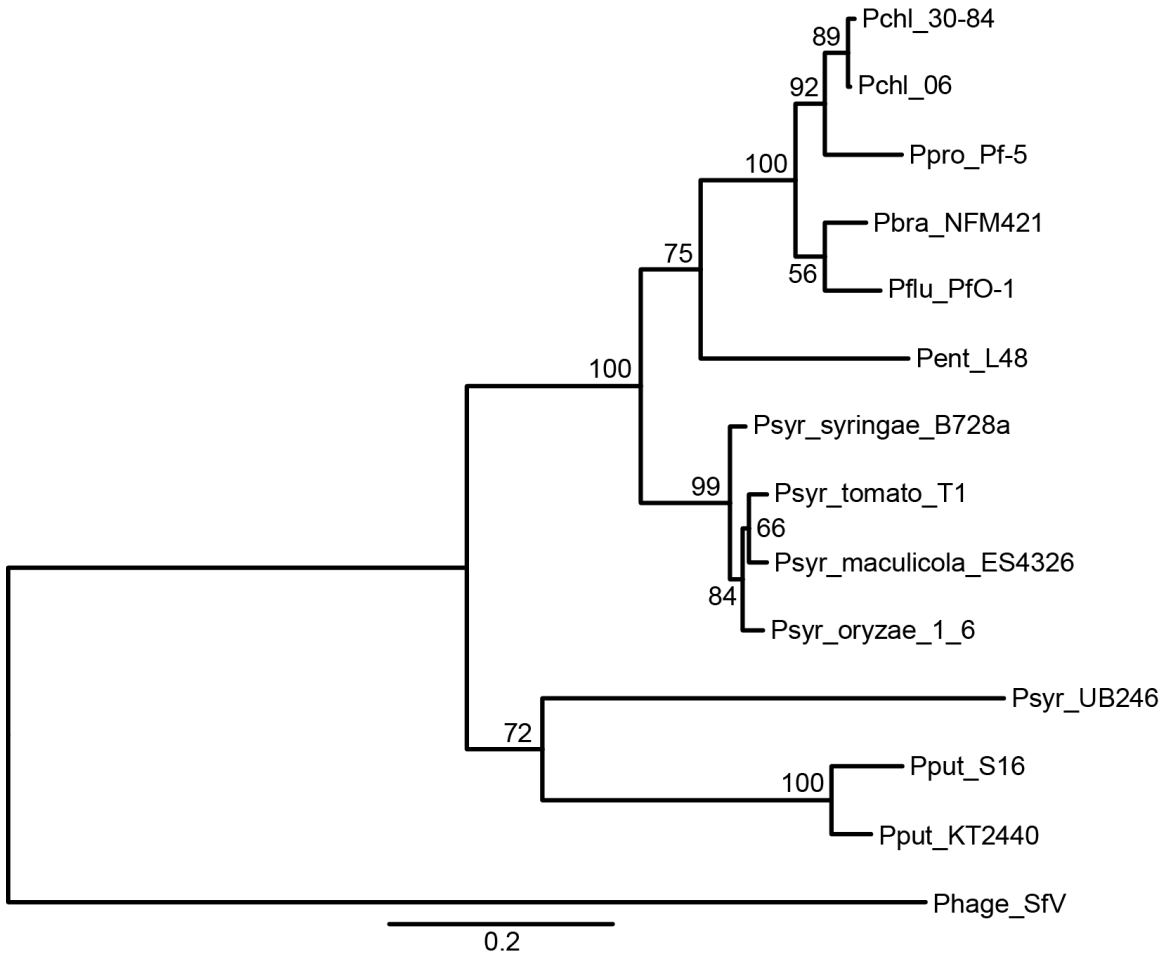

Figure S7. Maximum likelihood phylogeny of amino acid sequence of Psyr_4595 and its homologs from *Pseudomonas* strains harboring an R-type syringocin-like region. Values indicate bootstrap support (out of 1000 replicates, only values greater than 50 are shown). The following strains are Pchl_30-84 (*P. chlororaphis* 30-84), Pchl_O6 (*P. chlororaphis* O6), Pbra_NFM421 (*P. brasicacearum* NFM421), Pflu_PfO-1 (*P. fluorescens* PfO-1), Ppro_Pf-5 (*P. protegens* Pf-5), Pent_L48 (*P. entomophila* L48), Psyr_B728a (*P. syringae* pv. syringae B728a), Psyr_1_6 (*P. syringae* pv. oryzae 1_6), Psyr_T1 (*P. syringae* pv. tomato T1), Psyr_UB246 (*P. syringae* UB246), Pput_KT2440 (*P. putida* KT2440), Pput_S16 (*P. putida* S16). Phage_SfV (bacteriophage SfV, outgroup).

Table S1. R-type syringacin deletion strains.

Deletion Strain	Genes Disrupted	Annotation/Function[a]
ΔR_{reg}	Psyr_4603	RecA-mediated autopeptidase
	Psyr_4602*	Hypothetical protein
ΔR_{struct}	Psyr_4592[b]	Tape measure
	Psyr_4591	DNA circularization
	Psyr_4590	Baseplate hub
	Psyr_4589	Spike
	Psyr_4588	Baseplate
	Psyr_4587	Baseplate
	Psyr_4586	Baseplate
	Psyr_4585[b]	Receptor binding protein
ΔR_{rbp}	Psyr_4585[b]	Receptor binding protein
	Psyr_4584	Tail fiber assembly

*promoter of gene is removed, while coding sequence is unaltered in deletion strain.

[a] ΔR_{reg} annotations from IMG, ΔR_{struct} and ΔR_{rbp} annotations based on (Morgan et al. 2002; Leiman & Shneider 2012).

[b] Prediction based on synteny.

Table S2. Protein comparisons between *Psy* B728a R-type syringacin and prophage I from *P. protegens* Pf-5.

Psyr #	PFL #	% ID/%Similarity	% Query Coverage
4583	1227	68/76	100
4585	1226	61/66	8.6
4586	1225	70/85	100
4587	1224	71/85	99.4
4588	1223	58/73	100
4589	1222	76/90	89.4
4590	1221	61/76	91.4
4591	1220	52/70	47.7
4592	1219	30/46	71.6
4593	1218	75/86	85.7
4594	1217	69/80	100
4595	1216	79/90	100
4596	1215	58/75	95.2
4597	1214	51/64	99.0

Table S6. Strains and Plasmids

Strain or plasmid	Description or Relevant Charcteristics	Antibiotics	Reference
E. coli strains			
TOP10	F- *mcr*A Δ(*mrr-hsd*RMS-*mcr*BC) φ80*lac*ZΔM15 Δ*lac*X74 *rec*A1 *ara*D139 Δ(*araleu*) 7697 *gal*U *gal*K *rps*L (StrR) *end*A1 *nup*G		Invitrogen
DAB44	*E. coli* harboring pRK2013, (conjugation helper for triparental mating)		(Ditta et al. 1980)
P. syringae strains			
Pto T1	*P. syringae* pv. tomato T1		(Almeida et al. 2008)
Pla 106	*P. syringae* pv. lachrymans MAFF302278PT		(Baltrus et al. 2011)
Pto DC3K	*P. syringae* pv. tomato DC3000		(Buell et al. 2003)
Pmp	*P. syringae* pv. morsprunorum MAFF302280PT		(Baltrus et al. 2011)
Pan	*P. syringae* pv. actinidiae MAFF302091		(Baltrus et al. 2011)
Pja	*P. syringae* pv. japonica MAFF 301072 PT		(Baltrus et al. 2011)
Ptt	*P. syringae* pv. aptata DSM50252		(Baltrus et al. 2011)
Ppi	*P. syringae* pv. pisi 1704B		(Baltrus et al. 2011)
Psy B728a	*P. syringae* pv. syringae B728a		(Feil et al. 2005)
Pac	*P. syringae* pv. aceris MAFF302273PT		(Baltrus et al. 2011)
Cit7	*P. syringae* Cit7		(Baltrus et al. 2011)
Pla 107	*P. syringae* pv. lachrymans MAFF301315		(Baltrus et al. 2011)
Pta	*P. syringae* pv. tabaci ATCC11528		(Baltrus et al. 2011)
Pae	*P. syringae* pv. aesculi 0893_23		(Baltrus et al. 2011)
Pmo	*P. syringae* pv. mori MAFF301020		(Baltrus et al. 2011)
Pph 1448A	*P. syringae* pv. phaseolicola 1448A		(Joardar et al. 2005)
Pgy R4	*P. syringae* pv. glycinea A29-2		(Baltrus et al. 2011)
Por 1_6	P. syringae pv. oryzae		(Baltrus et al. 2011)
*Pcal**	*P. cannabina* pv. alisalensis		(Baltrus et al. 2011)
Δ0310	*Psy* B728a harboring a markerless deletion of Psyr_0310 and Psyr_0309		This study
Δ4651	*Psy* B728a harboring a markerless deletion of Psyr_4651 and Psyr_4652		This study
ΔS-type	*Psy* B728a harboring markerless deletions of Psyr_0310, Psyr_0309, Psyr_4651, and Psyr_4652		This study
ΔR_{reg}	*Psy* B728a harboring a markerless deletion of Psyr_4603 and the promoter of Psyr_4602 (Fig. S1)		This study
ΔR_{struct}	*Psy* B728a harboring a markerless deletion of Psyr_4586 through Psyr_4592 and the promoter of Psyr_4585 (Fig. S1)		This study
ΔR_{rbp}	*Psy* B278a harboring a markerless deletion of Psyr_4585 and Psyr_4584 (Fig. S1)		This study
ΔR_{reg} + pR_{reg}	ΔR_{reg} harboring pR_{reg} complementation vector (Kan^r, Fig. S1)		This study
ΔR_{rbp} + pR_{rbp}	ΔR_{rbp} harboring pR_{rbp} complementation vector (Tet^r, Fig. S1)		This study
Plasmids			
pJC531	Replicative destination vector harboring *attR* cloning sites	Kan^R	(Chang et al. 2005)
pMTN1907	Non-replicative destination vector harboring *attR* cloning sites	Kan^R, Tet^R, Cam^R, Suc^S	(Baltrus et al. 2012)
pDONR207	Entry vector harboring *attP* cloning sites	$Gent^R$, Cam^R	Invitrogen
pBAV226	Replicative destination vector with constitutive nptII promoter	Tet^R	(Vinatzer et al. 2006)
pR_{reg}	Psyr_4603 and Psyr_4602 plus flanking sequence in pJC531 (Fig. S1)		This study
pR_{rbp}	Psyr_4584 and Psyr_4585 complementation construct (including upstream alternative start codon) in pBAV226 (Figs. S1 and S2)		This study
pKLHECOEN3	Psyr_4585 and Psyr_4584 deletion construct integrated into pDONR207		This study
pKLHECODE5	Psyr_4585 and Psyr_4584 deletion construct integrated into pMTN1907		This study
pKLHECOEN11	R_{rbp} complementation construct integrated into pDONR207		This study
pKLHECOEN14	Psyr_0310 and Psyr_0309 deletion construct integrated into pDONR207		This study
pKLHECODE15	Psyr_0301 and Psyr_0309 deletion construct integrated into pMTN1907		This study
pKLHECOEN16	Psyr_4651 and Psyr_4652 deletion construct integrated into pDONR207		This study
pKLHECODE17	Psyr_4651 and Psyr_4652 deletion construct integrated into pMTN1907		This study
pKLHECOEN18	R_{struct} deletion construct integrated into pDONR207		This study
pKLHECODE19	R_{struct} deletion construct integrated into pMTN1907		This study
pKLHECOEN20	R_{reg} deletion construct integrated into pDONR207		This study
pKLHECODE21	R_{reg} deletion construct integrated into pMTN1907		This study
pKLHECOEN22	R_{reg} complementation construct integrated into pDONR207		This study

*Also known as *P. syringae* pv. maculicola ES4326

Table S7. Primers

Primer Name	Primer Sequence*
psyr_0310_E9_5'AS	GGCCTATTCCAGACTTAGGGTCCGCGAGCAAAAAATGGCAAGCCAGG
psyr_0310_E9_5'S	CAAAAAAGCAGGCTCCGCATTCGAGAAGTCGGTGATCGC
psyr_0310_E9_3'S	CCTGGCTTGCCATTTTTTGCTCGCGGACCCTAAGTCTGGAATAGGCC
psyr_0310_E9_3'AS	CCTGGCTTGCCATTTTTTGCTCGCGGACCCTAAGTCTGGAATAGGCC
psyr_4651_E9_5'AS	ATTTGTAGCGGGCAATGTTCTGTGACATGTCTTTCTCCTTGATTTGTG
psyr_4651_E9_5'S	CAAAAAAGCAGGCTCCGCTGTAGGCCCAGACGTAAGC
psyr_4651_E9_3'S	CAAGGAGAAAGACATGTCACAGAACATTGCCCGCTACAAATCAAGGCG
psyr_4603_5'AS	GCTTCAGAGACGCATGGTGAGAAAGTAGAAGCCGTGATGC
psyr_4603_5'S	CAAAAAAGCAGGCTCCCATCTGGAGCTCTGTGTATTCAC
psyr_4603_3'S	GCATCACGGCTTCTACTTTCTCACCATGCGTCTCTGAAGC
psyr_4603_3'AS	GAAAGCTGGGTGAGTTCGATGAACATTATCGCGC
$R_{struct.}$_5'S	CAAAAAAGCAGGCTCCGACATCATCACCGAGTCGATC
$R_{struct.}$_5'AS	CAGGCTGCTCACCACCATCGGCCCGATCACG
$R_{struct.}$_3'S	CGTGATCGGGCCGATGGTGGTGAGCAGCCTG
$R_{struct.}$_3'AS	GAAAGCTGGGTGGCGCGGTTAAGAAGCCC
B728a_4585/4584_KO_3'S	GACACGCCTAACGCAGTCCTTGCCGCTTGCCAAGCC
B728a_4585/4584_KO_3'AS	GAAAGCTGGGTGCGGTCGCGGCGTATATCG
B728a_4585/4584_KO_5'AS	GGCTTGGCAAGCGGCAAGGACTGCGTTAGGCGTGTC
B728a_4585/4584_KO_5'S	CAAAAAAGCAGGCTCCCAGGCGATCACGCAAAC
Rrbp_alt_start_5'S_C	CAAAAAAGCAGGCTCCCTTCAACTGAGGAACACAATGTGG
Rrbp_alt_start_3'AS_C	GAAAGCTGGGTGTTATAGTTCAAGTGAATTCGAGGGC
BP tailing primer F	GGGGACAAGTTTGTACAAAAAAGCAGGCTCC
BP tailing primer R	GGGGACCACTTTGTACAAGAAAGCTGGGTG

*All primer sequences read in the 5' to 3' direction (left to right). Sequence colored red indicates complementarity with primer used to amplify matching fragment. Sequence colored in blue indicates region where either BP tailing primer F or R can bind to prime in BP tailing PCR.